

Non Contact Test Points

**A high frequency measurement technique
for printed circuit boards**



Marcus Marmeheim

Division of Industrial Electrical Engineering and Automation
Faculty of Engineering, Lund University

LUNDS TEKNISKA HÖGSKOLA

NON CONTACT TEST POINTS

A high frequency measurement technique for
printed circuit boards

Marcus Marmeheim
2012

Supervisor: Gunnar Lindstedt
Examiner: Ulf Jeppson

Department of Industrial Electrical Engineering and Automation

ABSTRACT

A rising problem within electronics today is that, since the frequencies have increased dramatically, it is now very difficult to measure signals. If a traditional probe is used, then the direct contact will destroy the signal. The general idea behind this master thesis project is to make use of the crosstalk between transmission lines to create *non contact test points*.

This thesis aims to evaluate different designs, in order to optimize the crosstalk, and also make use of signal processing to recover the original signal.

Firstly, the problem was tackled with simulations and the results were analyzed in an attempt to optimize the design. Secondly, an actual circuit board was produced and the process was tested in reality.

It turned out that the idea of *non contact test points* was solid, and it is shown in the report that good measurements can be acquired with little effect upon the original signal.

NOMENCLATURE

Great efforts have been made to make this report accessible to the readers. Though all notations, abbreviations and acronyms should be described in the text, the most important ones have been listed below in an attempt to simplify the reading. It will be assumed that the reader is familiar with both the *SI base units* and the *derived SI units*.

NOTATIONS

Notation	Description
ϵ_0	Vacuum permittivity [$8.85418 \cdot 10^{-12} \text{ F} \cdot \text{m}^{-1}$]
ϵ_r	Dielectric constant []
$\mathbf{B}(x,y,z)$	Magnetic field [T]
c	Speed of light [$299\,792\,458 \text{ m} \cdot \text{s}^{-1}$]
C	Capacitance [F]
$\mathbf{D}(x,y,z)$	Displacement field [$\text{C} \cdot \text{m}^{-2}$]
D_0	see Figure 6.1 [m]
$\mathbf{E}(x,y,z)$	Electrical field [$\text{V} \cdot \text{m}^{-1}$]
f	Frequency [Hz]
F	Force [N]
f_s	Sampling frequency [samples $\cdot \text{s}^{-1}$]
G	Conductance [Ohm^{-1}]
I	Electrical current [A]
L	Inductance [H]
L_{out}	see Figure 6.1 [m]
L_{vic}	see Figure 6.1 [m]
$\mathbf{P}(x,y,z)$	Polarization density [$\text{C} \cdot \text{m}^{-2}$]
Q	Electrical charge [C]
R	Resistance [Ohm]
U	Electric potential [V]
W_{out}	see Figure 6.1 [m]
W_{source}	see Figure 6.1 [m]
W_{vic}	see Figure 6.1 [m]
Z_0	Characteristic impedance [$\text{Ohm} \cdot \text{m}^{-1}$]
α	Attenuation constant []
β	Phase constant []
γ	Propagation constant []
λ	Wavelength [m]
Z	Impedance [Ohm]
ρ	Reflection constant []
μ_0	Vacuum permeability [$4\pi \cdot 10^{-7} \text{ V} \cdot \text{s} \cdot (\text{A} \cdot \text{m})^{-1}$]

ABBREVIATIONS AND ACRONYMS

Abbreviation	Description
.s*p	A Touchstone file, designed to store S-parameter data
BPC	Board Platform Cadence
CAD	Computer Aided Design
DUT	Device Under Test
EAB	Ericsson AB
EM	Electro Magnetism
GUI	Graphical User Interface

IC	Integrated Circuit
IEA	Division of Industrial Electrical Engineering and Automation LTH Faculty of Engineering, Lund University
LTH	Lunds Tekniska Högskola (Lund University's faculty of engineering)
NCTP	Non Contact Test Points
PCB	Printed Circuit Board
SMA	A connector type
SMP	A connector type

TABLE OF CONTENT

Abstract	2
Nomenclature	3
<i>Notations</i>	3
<i>Abbreviations and Acronyms</i>	3
1. Project description	7
2. Introduction	8
<i>Preface</i>	8
<i>Project overview</i>	9
3. About Ericsson	10
4. Theory	11
<i>Electromagnetism</i>	11
<i>Transmission lines</i>	13
<i>Printed circuit boards</i>	17
<i>System theory</i>	18
<i>Square waves</i>	19
<i>Vector pole fitting</i>	21
<i>Measurement theory</i>	21
<i>Embedding and de-embedding signals</i>	23
<i>The Project</i>	24
5. Design introduction	26
6. Simulation	27
<i>Other structures</i>	34
7. Implementation	36
<i>Introduction</i>	36
<i>Chosen designs</i>	36
<i>CAD (computer aided design)</i>	38
<i>Encountered problems</i>	39
8. Signal processing	41
<i>Theoretical approaches</i>	41
<i>Testing the principle</i>	43

9. Measurements	48
<i>S-Parameters</i>	48
<i>Using the reconstruction software</i>	50
10. The final program	54
<i>Non Contact Test Point ANALYZER</i>	54
11. Conclusions	56
<i>The project</i>	56
<i>Future work</i>	56
References	58
Appendix A.....	61
<i>SCXB</i>	61
Appendix B.....	62
<i>SMP-connector test board</i>	62
Appendix C.....	63
----- <i>User's guide</i> -----	63

1. PROJECT DESCRIPTION

The main goal of this project was to create a possibility to perform high frequency measurements within a printed circuit board. This was to be done by building a small transmission line next to measurement point in order to generate crosstalk and then, by analyzing the crosstalk, reconstruct the original signal.

The main objectives were the following

- Optimizing the geometries for the circuit by the use of simulation
- Implementing the chosen design in an existing PCB (printed circuit board)
- Making comparisons between the simulations and the actual circuit
- Doing the necessary measurements and calculations to embed and de-embed the signal
- Building a software, capable of reconstructing the original signal, and implementing it in an oscilloscope

Since the project was created, and funded, by the Swedish telecom company Ericsson, it was done at one of their departments in Stockholm. Apart from the objectives above, the completion of the project would also require extensive use of simulation software, network analyzers, oscilloscopes and MATLAB. Also there was a wish by Ericsson to have the results explained by text book theory, to the furthest possible extent. Additionally, an internal report with detailed instructions on how to build these test points was requested as well as a description of how to use the created GUI.

2. INTRODUCTION

PREFACE

The idea behind this thesis project was not my own, I simply applied to an open position at *Ericsson*. Instead the credit for inventing it belongs to Ingvar Karlsson, a senior specialist within signal integrity and EMC at the company. He came to be my supervisor during the semester, and I would like to state my sincerest thanks for his invaluable help during this endeavor.

My university supervisor was Gunnar Lindstedt, an associate professor and my examiner was Ulf Jeppsson, also an associate professor. Both of them belong to the department of *Industrial Electrical Engineering and Automation*, and I am very grateful for their support and feedback as well.

This is a thesis for a master's degree in science engineering of physics at *Lunds Tekniska Högskola (Lund University, Faculty of engineering)*. Though the thesis in many ways relate to physics, the subject covered also include electrical engineering, signal processing, measurement techniques, signal integrity and applied mathematics. Most necessary theoretical knowledge will be introduced to the reader within the report, it is only necessary to have some very basic understanding of the subjects mentioned. However, it was from start my intention to only cover the required information and try not to divert the attention from the main goal. For example; the physical effect of not terminating a transmission line properly is described, but an explanation of why that happens is not included.

The report is not written in a very typical way, the chapters were created to somehow mirror the working process of the project. Though there is a chapter called *Theory*, it only covers the text book theory of this project. Instead the reader will be introduced to necessary information, when that necessary knowledge is needed. In many ways this was how the project was done, I did not consider how to calibrate the S-parameters of an input until that task was faced.

The same can be said about the results and conclusions; they are usually included in the same chapter as they are produced. For instance; the results of each simulation is described in the same place as the simulation variable setup. The conclusions and results are also included directly.

From the first day at the company, it was clear that I might be fighting a losing battle. Many other engineers had doubts whether this project would be a success and some questioned even if it was feasible to begin with. Still I would like to direct my thanks to the department as well, for I could always rely on skilled support when needed. Two people worthy of honorable mentions are Stephen Grant-Davies (the CAD-specialist that put up with all my unorthodox requests) and Madeleine Baumann Ahlzén (the section manager that gave me this opportunity to begin with).

I hope that this thesis will bring some new knowledge to the art of PCB design, and that the readers will find the information valuable and interesting.

Best Regards,

Marcus Marmeheim, M.Sc Engineering physics student, LTH

PROJECT OVERVIEW

In order to prepare the reader for the following parts of the report, this section was added to offer a better overview of the project than the one found under *Project description*. Roughly characterized, the project followed this structure:

- **Theoretical assumptions/simulations**

By the use of theory and simulations, the optimal geometries for the test points would be pursued. The work done during this part of the thesis project is described in the chapters *Theory* and *Simulations*.

- **Implementation**

This part consisted of using CAD tools to implement the created structures upon an actual circuit board. It is described by the chapter *Implementation*.

- **Building a software**

Creating a software (with a user friendly GUI) was a work that was carried on for a long time. It involved; choosing the mathematical procedure on how to recreate the signal, evaluating the performances, building a GUI that was easy to use and implementing additional features in it.

Because of the many stages of this part, there is no separate chapter that describes this entire task. Instead descriptions can be found in the following chapters: *Signals processing*, *The final Program* and *Appendix C* (where the software's User's guide has been included).

- **Verification and evaluation**

After the implementation was done, it was time to evaluate the results. The work consisted of checking transfer functions and studying how well the software was able to perform its task of reconstructing the signal. All of this is described in the *Measurements* chapter.

3. ABOUT ERICSSON

For a long time *Ericsson AB* (sometimes denoted as EAB) has had a special place among Swedish companies. Though many huge multinational companies originate from Sweden, *Ericsson* has made itself a symbol for the new and modern IT industry.

Outside of Sweden the corporate name *Ericsson* may not be as famous. Many may confuse it with its daughter company *Sony Ericsson* (co-owned with *Sony*), that develops cell phones. This is probably due to that not many consumers come in direct contact with *Ericsson* products. Even in Sweden, where most know of the company's existence, not everyone would be able to say what it actually does.

However, though direct contact with the products may be uncommon, people would probably be surprised by how dependent they are on the company. If a person picks up a random cell phone somewhere in the world and places a call, by 40% likelihood, it will go through a telecom network designed by *Ericsson*.

This is the very core of *Ericsson's* business, and thanks to the boom of information technology, it has made the company one of the world's leading powerhouses of technology. Business has since long been expanded beyond simple phone services and today the company also researches and develops new broadband, multimedia, and software technologies. Apart from development and manufacturing, *Ericsson* is also able to provide management and service for delivered systems.

It all started in 1876, when *Lars Magnus Ericsson* opened a small repair shop for telegraphs. Located in Stockholm, Sweden, business quickly soared and only five years later the company had expanded enough to win contracts outside of Sweden as well. Still today, Stockholm is the base of *Ericsson's* operations, though most of the actual manufacturing has been moved abroad.

The rapid expansion continued, and 25 years later the company staff consisted of more than a thousand employees. Throughout the following century, business kept growing and reached a peak during the IT-boom of the early 2000's. After the industry's subsequent crash landing, the company lay off a huge part of its workforce, but has since then returned to growth.

Today around 90 000 employees work for *Ericsson*, and several thousand others for partly or fully owned subsidiaries. The company operates worldwide and serves clients in more than 180 countries.



4. THEORY

ELECTROMAGNETISM

INTRODUCTION

Electromagnetism is an incredibly broad field within physics, and to give a fairly good coverage of it would require an amount of text capable of filling several books.

This short section aims just to give some basic introduction, and the necessary information to understand this thesis.

ELECTRIC FIELDS

An electric field is a result of charges, and it is dependent on the charges positions, velocities and accelerations.

If one of the field lines is studied, it will start at one of the positive charges and propagate towards a charge with opposing sign, towards ground or just away from the charge towards infinity. It is also possible for the field line to start at infinity or ground and propagate towards a negative charge. Figure 4.1 below gives an example.

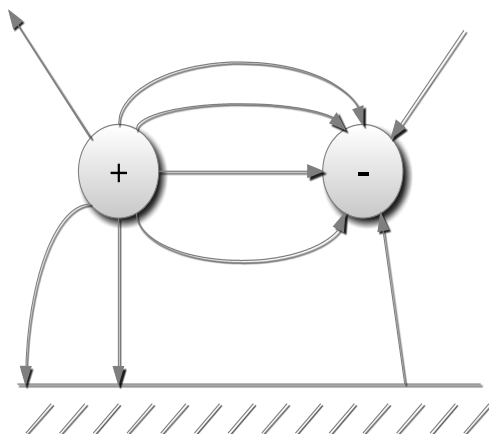


Figure 4.1. A schematic view over how the field lines of an electric field will look. The thick black line in the bottom of the picture symbolizes ground.

Another interesting fact is that the difference in electrical potential $V(r_{12})$ between two points (p_1 and p_2) in space is equal to the integrated electrical field (\mathbf{E}) along any trajectory between them, according to (4.1)

$$V(\mathbf{r}_{12}) = - \int_{p_1}^{p_2} (\mathbf{E})dl \quad (4.1)$$

If the fact that a charge (Q) within an electric field also is subjected to a force (\mathbf{F}), described by (4.2), is taken into account then it is apparent that there is a difference in electrical potential energy depending on whether the charge resides in p_1 or p_2 .

$$\mathbf{F} = Q\mathbf{E} \quad (4.2)$$

This means that the potential electrical energy may be converted into kinetic energy, if the charges are free to move. Since electric potential is the same as voltage and moving electrons the same as current, it is now clear that a voltage has the ability to produce a current.

It is not an uncommon belief that currents propagate at the speed of light, but this is only partly true. The charges do not propagate at such speed, in fact very far from it, but the electric field does when passing through vacuum, in other materials the speed will be changed. That should not be surprising, considering that light is simply electromagnetic radiation. This gives the effect that if you create a current through an object, and measure the amount of charges that exits at one end, then the charges will start to arrive at the same time as the electric field no matter how big the object is.^{1,32}

CONDUCTORS AND INSULATORS

It is common knowledge that every material contains positive and negative charges (protons and electrons), but not all materials will be able to support a current. It was

mentioned in the previous section that a current is dependent on the charges ability to move, and that ability will be dependent upon which material they reside within. If the charges are bound to each other, then a current will not appear, and the material will be classified as an insulator. But if the electrons (it is the electrons that physically move) are able to leave the atom structure, they may form a current. If the ability to support a current is strong enough, then the material will be classified as a conductor. The parameter *conductivity* is used to describe how well a material conducts a current, and it is specified by Siemens per meter (Sm^{-1}). Conductors are materials with high conductivity.

A very common conductor, within electrical engineering, is copper. Its conductivity is about $5.8 \cdot 10^7 \text{ Sm}^{-1}$ and it was the conductor used exclusively during this master thesis project.

This can be related to circuit theory; the conductivity of a conductor is proportional to the inverse of its resistance. It should also be mentioned that the geometries of the conductor changes the resistance; if the width and height of the conductor are constant along its propagation, then its resistance will be inversely proportional to the area of its cross section. There are, of course, other variables that affect the resistance, but these do not need to be explained in the theory section of this thesis.^{1,3,4}

DIELECTRIC MATERIALS

Dielectrics are insulators with the ability to polarize. This means that the charges within the atoms can regroup when exposed to an electrical field. In figure 4.2 below, the effect is shown. In reality most insulators show this ability, but to a varying degree. They are used

in PCB (printed circuit board) design, and this effect must therefore be considered.

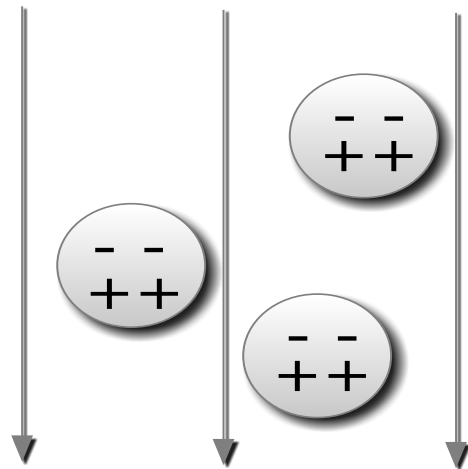


Figure 4.2. A schematic description of how the charge densities within atoms (symbolized by circles) change when exposed to an electrical field.

When this happens, the charges themselves will create an electrical field that counteracts the original field.

Usually this effect is described by the polarization field, \mathbf{P} , and it is proportional to \mathbf{E} . The displacement field, \mathbf{D} , is a combination of both \mathbf{P} and \mathbf{E} , and it is described by the relation (4.3) below. Note that \mathbf{P} is not just the electrical field that counteracts \mathbf{E} , it is a description of the electrical dipole moment that has been forced upon the atoms. The displacement field then, in turn, describes the field that is created because of the forced separation of charges.

$$\mathbf{D} = \mathbf{P} + \epsilon_0 \epsilon_r \mathbf{E} \quad (4.3)$$

Further effects and implications of this relation will not be explored in this thesis, since they are not relevant for the project. But the constant, ϵ_r (called dielectric constant), is. It is a dimensionless constant that will have a tremendous effect upon applied conductors. This is because the propagation speed of an electric field, V_E , through a conductor is affected, according to (4.4), by the dielectric materials surrounding it.^{1,34}

$$V_E \sim \frac{1}{\sqrt{(\epsilon_r)}} \quad (4.4)$$

MAGNETIC FIELDS

It turns out that there is a connection between the electric forces and the magnetic forces, but these will not be derived in this thesis. What is important is that moving electrical charges (creating a current \mathbf{I}) will generate a magnetic field (\mathbf{B}), and that field can (for a long, thin conductor) be calculated by the *Biot-Savart law* (4.5). μ_0 is a constant relating to theory not necessary for this thesis.

$$\mathbf{B} = \int \frac{\mu_0 I d\mathbf{l} \times \mathbf{r}}{4\pi |\mathbf{r}|^3} \quad (4.5)$$

\mathbf{r} is the point where the field is measured. It should be noted that the magnetic field around a thin circular conductor is shaped symmetrically around it, and that it is proportional to $\frac{1}{r}$.

There is also a possibility to create the opposite effect and have a current generated by a magnetic field. This effect is called induction, and it is dependent on the field's fluctuation.

If a conductor is suddenly exposed to a magnetic field (B_1), it creates a current that is directed so that the magnetic field (B_2) it creates counteracts the original field. But if B_1 is kept constant, the induced current will decrease and eventually disappear. If there is to be a constant current in the conductor, the field needs to constantly fluctuate. There are analytical ways to calculate this effect but in this thesis a more practical approach will be taken, mainly via simulations. This is because the geometries of the conductors used in this project would create severe difficulties for an analytical approach.¹

TRANSMISSION LINES

THE BASICS

In basic circuit theory, the lines connecting the different components have no significance. Hence, Ohm's law may be applied directly to the linear elements. However, that approximation is only valid when the wavelength is much larger than the length of the circuit. As the frequencies (f) in IC:s (integrated circuits) and PCB:s increase, the wavelengths (λ) decrease proportionally according to (4.6), where c equals the speed of light

$$c = \lambda f \quad (4.6)$$

This has resulted in the need to apply *transmission line theory*, instead of ordinary circuit theory, when studying modern IC:s.

A transmission line is usually modeled as in figure 4.3 below. It has two different conductors that are interconnected by several resistors and capacitors. Additionally, each conductor contains resistors and inductors. Usually one defines the characteristics of a transmission line by identifying the parameters C_0 (capacitance per unit length), L_0 (inductance per unit length), G_0 (conductance per unit length) and R_0 (resistance per unit length). This allows you to easily see how the length of a transmission line will impact its performance.

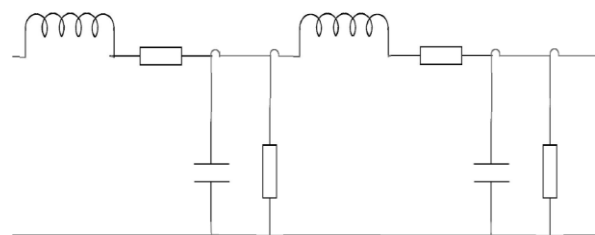


Figure 4.3. A model for a transmission line.

Both the conductors carry the same amount of current, but in opposite directions, effectively closing a loop. It should be noted that it is also possible to let ground act like the second conductor. By using the parameters above, it is possible to define the characteristic impedance, Z_0 , according to (4.7) below. This is an important variable for both the transmission line theory and this thesis as a whole.^{2,3,4,7}

$$Z_0 = \sqrt{\frac{R_0 + j\omega L_0}{G + j\omega C_0}} \quad (4.7)$$

PROPAGATION AND ATTENUATION

Another important variable, definable by the same parameters, is the wave propagation constant γ . It describes the wave propagation through a transmission line, and it is defined by (4.8)

$$\gamma = \sqrt{(R_0 + i\omega L_0)(G_0 + i\omega C_0)} \quad (4.8)$$

It is now easy to see that (as long as no parameter is equal to zero) γ may be written as (4.9), and the entire electromagnetic wave propagation through a transmission line may be approximated by (4.10)

$$\gamma = \alpha + \beta j \quad (4.9)$$

$$V(z) = e^{\gamma z} \quad (4.10)$$

If (4.9) is compared to (4.10) it quickly gets apparent that β is dependent on the frequency, which is not very surprising considering that it (because of j) describes the phase of the wave. But α , which is called attenuation constant, seems to be completely independent of the frequency, implying that a signal propagating through a transmission line is attenuated the same amount no matter what its frequency is.

If this conclusion was to be tested in reality, it would not hold up very well. It turns out that every parameter in (4.8) is frequency

dependent. To completely derive this effect for every parameter was not a necessity for this thesis, but since the attenuation caused by R_0 and G_0 would play major roles in this project they are examined in the following sections.^{1,4}

DIELECTRIC LOSSES

A simplified way to put it is to say that the frequency dependency of R_0 relates to the *skin effect* and that of G_0 to dielectric losses. The dielectric losses come from the field surrounding a transmission line in a dielectric material. Every time that the field changes, so do the local charge densities within the atoms (see earlier parts off the *Theory* chapter), and each time, a small amount of energy is lost during the process. Since the electric field oscillates with the same frequency as the signal frequency, it is logical that a higher frequency will generate a higher loss of energy.^{1,4}

It turns out that the dielectric losses are proportional to the frequency of the signal, according to (4.11)⁷

$$G_0 \propto f \quad (4.11)$$

SKIN EFFECT

There is an effect, when current travels through a conductor, which is called *skin effect*. Its name comes from the fact that the current is located close to the surfaces of the material, and this is because the charges repel each other.

If a cross section of the conductor is observed, the charge density (J) would decrease with the distance (d) from the surface according to (4.12)

$$J \propto e^{-\frac{d}{k}} \quad (4.12)$$

k is a term, that relates (among other things) to the frequency of the signal. Since the area of a cross section (that carries the current) decreases due to the skin effect, the resistance of the conductor increases (as described earlier in the chapter). If more advanced calculations were to be made, it would turn out that a good approximation for the relation between the R_0 and the frequency is (4.13).

$$R_0 \propto \sqrt{f} \quad (4.13)$$

Since R_0 and G_0 make up the real term α in γ , the frequency dependent attenuation of a transmission line has now been explained. ^{4,7}

REFLECTION

One important aspect of transmission lines is the difference in behavior, depending on how they are terminated. First we must realize that in transmission lines the phase of the signal will vary along its propagation. This is the main reason for the need to apply transmission line theory.

The effect that will come into play when choosing a termination is called *reflection*. It is governed by the general law (4.14) below

$$\rho = \frac{Z_L - Z_0}{Z_L + Z_0} \quad (4.14)$$

ρ is a dimensionless constant (possibly complex) that describes how much of a signal that will be reflected backwards when encountering a termination.

The observant reader may have already identified that there are three extreme cases;

- $Z_l = Z_0$:
Nothing will be reflected backwards, the entire signal propagates forward.
- $Z_l = 0$ (*short circuited*):
The entire signal will be reflected backwards, but with negative relative amplitude.

- $Z_l = \infty$ (*open ended*):
The entire signal will be reflected backwards, with its original structure.

Of course, (4.14) also predicts that there will be an infinite number of different possible values for ρ . However, though infinitely many values are possible, all of them reside within $[-1,1]$. ^{4,8,10}

STUBS

In transmission line theory, a stub is a very short section of a transmission line that branches away from the main line. In figure 4.4 below, this is shown schematically. The stub can, as depicted, be an open ended extension or a short circuit between the two different signal paths (like always, in transmission line theory, it is possible to let ground act like the second path).

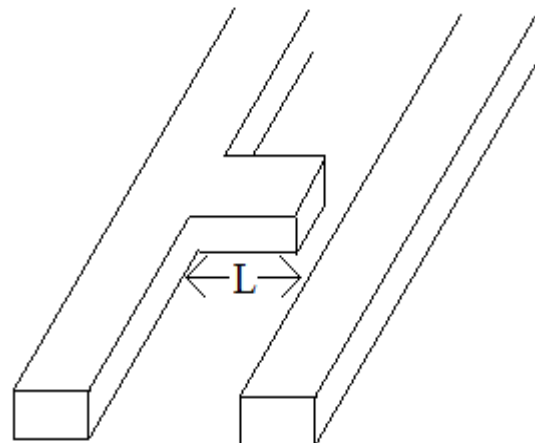


Figure 4.4. A schematic description of an open ended stub with length L . If the stub was short circuited, the two conductors would be connected by the stub and L would be equal to the distance between them.

From the main circuit, stubs will look like different impedances depending on if they are open or short circuited. Open circuited stubs have the input impedances described by (4.15)

$$Z_{in} = -jZ_0 \cot(\beta L) \quad (4.15)$$

and short circuited stubs have input impedances described by (4.16)

$$Z_{in} = jZ_o \tan(\beta L) \quad (4.16)$$

Both input impedances are approximations, since the real valued impedances are not included. This makes the impedance of the stubs look purely imaginary, and frequency dependent.

Though there are several uses for stubs within electrical engineering, they can often cause problems if created unintentionally. Since they have different effects upon different frequencies, they are able to distort a signal.⁴

CROSSTALK

The basic concept of crosstalk is that a change in voltage level in one transmission line will generate a voltage pulse in another. There are two physical reasons why this happens: capacitive coupling; and inductive coupling.

The principle of capacitive coupling is very much related to that of a capacitance. If there is a voltage difference between the lines, then a current (and thereby also a voltage) will be generated in the second line according to figure 4.5 below. Just like in the case with an actual capacitance, the current in the second transmission line will eventually cease if the voltage level in the upper line stabilizes.

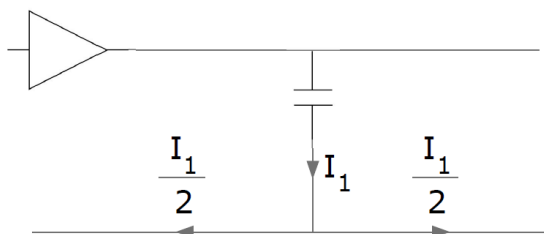


Figure 4.5. A circuit model for the capacitive coupling effect. It should be noted that the current I_1 , upon reaching the second conductor, splits in two current, both of equal size but traveling in opposite directions.

Inductive coupling is the voltage induced in the second transmission line due to a fluctuating magnetic field, generated by changes of the signal levels in the first one. The two pictures (figure 4.6 and figure 4.7) below describe the current generation in a magnetic field and a model for the behavior using circuit theory.

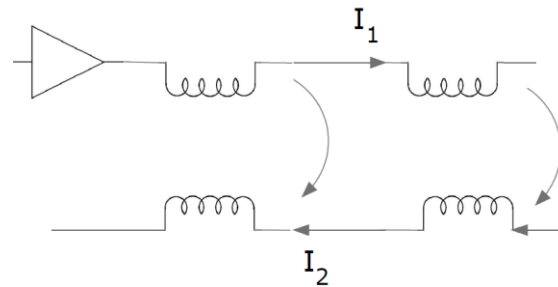


Figure 4.6. The current I_1 will generate a magnetic field, that will induce the current I_2 in the second conductor.

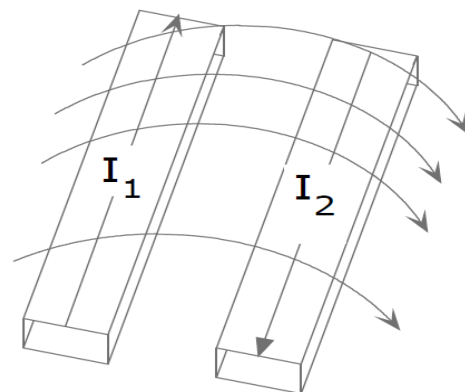


Figure 4.7. One conductor's current (I_1) generates a magnetic flow, that in turn generates a current (I_2) in the second conductor.

It is important to note that, when observing inductive coupling, current is generated backwards (i.e. in opposite direction of I_1 , as can be seen in figure 4.6 above). If the two coupling procedures are combined we end up with a more complex model depicted in Figure 4.8 below.^{8, 10}

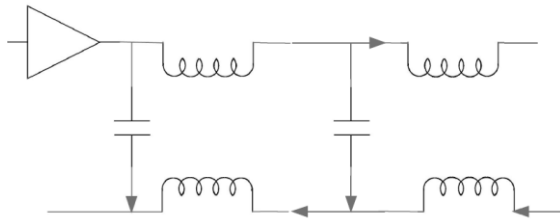


Figure 4.8. The circuit model for crosstalk between two conductors. Both the capacitive coupling and the inductive coupling effects are included.

PRINTED CIRCUIT BOARDS

BASICS

The printed circuit board (PCB) dates back to the 1940's. Its main purpose is to connect different electronic components, and also provide a steady structure. Though expensive to design, they are easy to mass produce and are considerably more reliable than the option of having free wires between the electronic components. Originally, the board consisted of a single layer of copper threads (or traces) that was imbedded in a dielectric material. As science and technology advanced, there came a need for more complex board structures. The solution was to start producing multilayer boards. A schematic model for a simple board is given in figure 4.9 below.^{9, 34}

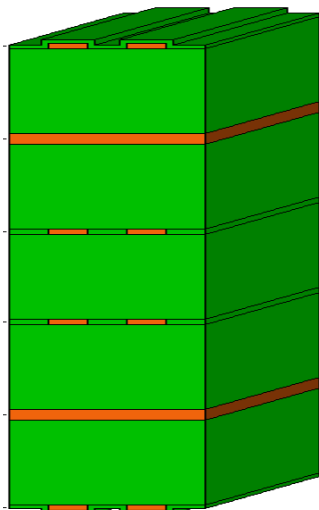


Figure 4.9. A schematic cross section for a PCB (generated by use of HyperLynx from Mentor Graphics Corporation). The orange color represents conductor materials, while the green color is dielectric material. The two thick orange layers are used as planes conducting a reference voltage or acting as ground, while the four layers, containing two separate conductors, are layers where the signals are propagated (commonly called signal layers).

INTERNAL CONDUCTORS

Usually signals in a PCB are propagated via two parallel conductors (just as depicted in figure 4.7), and these two may be in *common mode* or *differential mode*.

In *common mode* the conductors are fed the same voltage, while in *differential mode* they are fed the same amount of voltage but with opposite signs (e.g. 40mV and -40mV respectively).

It is common practice to always choose *differential* over *common mode*. The reason for this relates back to physics. Since the total magnetic field, generated by the two conductors, is a superposition of each one's separate field we end up with two very different options. The reason *common mode* signal even exists are through faults in the design; e.g. they may be added upon another signal by disturbances.

As can be seen in figure 4.10 below, most of the magnetic field is cancelled in *differential mode*, while it is severely increased for *common mode*. It is of course always desirable to decrease the magnetic fields within a PCB, since this also will decrease the amount of crosstalk.^{9, 29, 34}

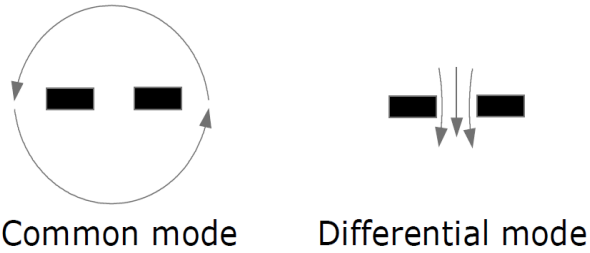


Figure 4.10. The resulting magnetic fields generated by a pair of transmission lines in common mode and another in differential mode.

VIAS

Vias are used in order to connect different signal layers. They consist of a drilled hole through the PCB where the walls have been covered in conducting materials. It is thereby easy to connect certain layers to the *via*, simply by letting two conductors come into contact with the walls. A schematic example is given in figure 4.11.

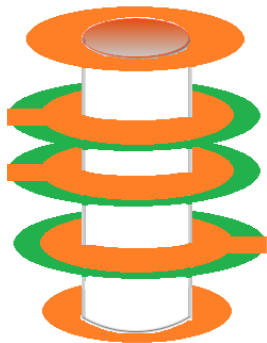


Figure 4.11. Schematic example for a *via*, like earlier, the conducting materials are symbolized by orange and the dielectrics by green.

Even if the top or bottom layers are not connected to the *via*, it is still common to make the hole through all the layers. The reason for this is practical, as it otherwise complicates production (and therefore increases costs). But there are other types of vias; a *blind via* is only connected to one surface layer, a *buried via* is completely contained within the structure and a *micro via*

is a *via* that is very small (even by PCB standards).

However, there may be a lot to gain by only making the *vias* as long as the distance between the layers it is connecting. If there is a segment of the *via* that is completely redundant, it may act as a stub and pose a serious threat to the signal integrity.^{7, 8, 29, 34}

SYSTEM THEORY

INTRODUCTION

System theory is a widely used term within the scientific community, and it may apply to a great variety of different subjects. The system theory covered in this section will strictly relate to the *Linear time invariant system theory*, which is a form of applied mathematics.

It is not intended, for this thesis, to give a full coverage of system theory, but some basic knowledge will be necessary to understand the later chapters.

TIME AND FREQUENCY DOMAIN

A very basic and important concept, within this theory, is that almost any time dependent function, $g(t)$, may be approximated by the sum of several different trigonometric functions. In (4.17) the reader may see how this works

$$g(t) = \frac{a_0}{2} + \sum_{n=1}^{\infty} \left(a_n \cos\left(\frac{n\pi t}{T}\right) + b_n \sin\left(\frac{n\pi t}{T}\right) \right) \quad (4.17)$$

The bigger the amount of frequencies that are included in the series, the more exact the approximation will become. (4.17) gives the possibility to describe a time dependent function by how strong the frequencies, that it contains, are. This is

commonly referred to as frequency representation of a time dependent function.

It is also possible to create a system, based upon desirable frequency properties. For instance, to create a low pass filter one defines in what way it will amplify or decrease specific frequencies.

The system can then be used to operate upon signals, either in frequency domain or by the use of its time domain representation (called impulse response). How to convert the representations from one domain to the other will not be discussed further in this thesis. For a greater understanding, the reader is encouraged to study any literature on the matter.³³

CONVOLUTION

The method to describe a system's operation upon a signal mathematically is to convolve the signal with the impulse response of the system. An exact analytical description, of a convolution between $f(t)$ and $g(t)$ is given in (4.18) below

$$f(t) * g(t) = \int_{-\infty}^{\infty} f(\tau)g(t - \tau)d\tau \quad (4.18)$$

However, it is also possible to perform the operation in frequency domain. If we let $F(f)$ and $G(f)$ denote the frequency domain representations of the functions, then the operation is simply a scalar between the two.³³

$$f(t) * g(t) = F(f) \cdot G(f) \quad (4.19)$$

S-PARAMETERS

If you connect two transmission lines to the same black box, as depicted in figure 4.12 below, you will be able to measure the S-parameters (or scattering parameters) of the box. These parameters are simply the

input/output relations at different frequencies, and they are very commonly used within electrical engineering.

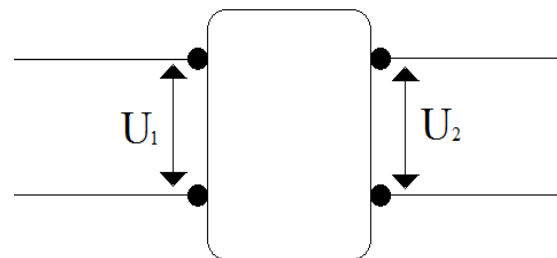


Figure 4.12 A two port, with the voltages U_1 and U_2

What makes the S-parameters different from a simple frequency response, used in disciplines like control theory, is that they will also tell how much of the input signal that will be reflected backwards.

The complete structure for the S-parameters, of the 2-port depicted earlier, is given in (4.20)

$$S = \begin{pmatrix} S_{11} & S_{12} \\ S_{21} & S_{22} \end{pmatrix} \quad (4.20)$$

Here S_{12} is the transfer function (in frequency domain) from U_2 to U_1 , and S_{21} is of course the transfer function in the opposite direction. S_{11} and S_{22} describe how much of the input signal that will be reflected backwards on each respective side.

It is of course possible, using S-parameters, to describe systems with more than 2 ports. The S-matrix will then be expanded accordingly, but the principle will remain the same.

One should keep in mind that the parameters are complex-valued, in order to capture the phase shift of the signal.⁴

SQUARE WAVES

INTRODUCTION

The name, *square waves*, gives a good description of what their appearance is like.

They are shaped like rectangular blocks, and an example is given in figure 4.13 below.

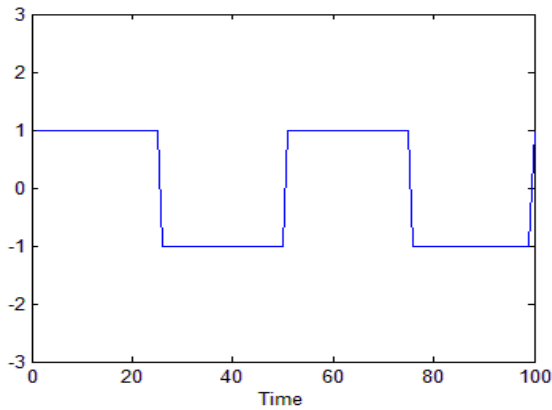


Figure 4.13. A simulated periodical square wave.

Though they are not that interesting from a mathematical point of view, they have come to play a vital role within modern electronics. Since digital systems view information as *ones* and *zeroes*, square waves have become a good way of propagating the information. If intervals are defined in a way that makes the value of the signal constant almost everywhere within them, then the values may be interpreted as a *one* or a *zero*. If also the signal is manipulated to represent the information, the result will be a signal that propagates the desired information. An example of this is given in figure 4.14 below.

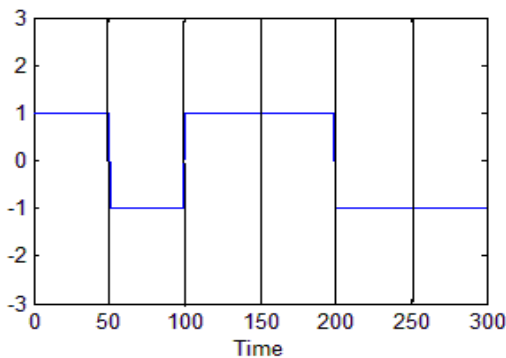


Figure 4.14. The figure shows an example of information propagation by the use of square waves. The intervals have the length 50 time units, and if the signal has the value 1 within the interval it is interpreted as a one. If it has the value -1, it is

interpreted as a zero. Hence; the information transmitted in this simulation would be [101100].

As can be seen in figure 4.14, it is not necessary to make the signal value 0 relate to the bit *zero*. Neither would it be necessary to make the signal value 1 relate to bit *one*. What is important is consistency, so that the information will be interpreted correctly. As mentioned previously, the signals within a PCB is made up of voltage.^{8, 33}

MATHEMATICAL ANALYSIS

Within theoretical mathematics it would of course be entirely possible to make the derivatives of the slopes approach infinity, effectively making the slopes almost perfectly vertical. But if the theory is applied, the slopes will create rise and fall times for the signals. These time intervals will come to play a vital role when analyzing the frequency content of a signal.

In theory it would take an infinite amount of frequencies to approximate a square wave completely (see (4.17)), but in reality most of the frequency content will be localized close to 0 Hz. There is a way to approximate what frequency span most of the signal resides within; if the rise and fall times (t_0) of the wave are equal and the length of an interval is t_{int} , then most of the signal content (S_m) is found in the interval described by (4.21).

$$\frac{1}{\pi \cdot t_{int}} < S_m < \frac{1}{\pi \cdot t_0} \quad (4.21)$$

If this theory is applied to the real values of this project, it is possible to predict at what frequencies the measurements will take place. Since the board, that we will apply the circuit upon, propagates data at 10Gbit/s the period length for a single bit is

$$\frac{1bit}{10Gbit \cdot s^{-1}} = 0.1ns$$

t_0 , on the other hand, can vary a bit. But according to specifications it is bound between 24ps and 47ps, and in this project it was approximated to 35ps.

This means that the frequency span, for the applied circuit, between 3.2GHz and 9.1GHz will contain most of the signal information. However, though the interval contains most of the content, there is still much content to be found below 3.2 GHz. Hence, it is the upper limit that is most important.

One last thing to point out is that when the information speed increases, the rise and fall times always decrease. This means that the frequency span will get wider, and that higher frequency content will be found in signals with a higher bit/s ratio.³³

VECTOR POLE FITTING

Vector pole fitting is a relatively new way of approximating a transfer function. It was developed to be used by computers, capable of performing heavy calculations.

BASIC PRINCIPLE

It may sound simple to approximate a transfer function accurately, since many text books describe them as simple analytical functions of low degrees. In reality, it is seldom as simple as that. If a real system is analyzed, the transfer functions often look far more chaotic than in the made up scenarios. This makes it very difficult to use analytical approaches for estimations and such.

The idea behind *vector pole fitting* is to approximate any transfer function simply by placing poles in appropriate positions. This would work in the way described by (4.22). $f(s)$ describes the real transfer function, and, except s , all letters are constants.

$$f(s) \approx \sum \frac{c_n}{s - a_n} + d + sh \quad (4.22)$$

How this approximation is done is not a trivial thing. For this thesis it will be enough to say that this approximation often works quite well. Another important aspect of *vector pole fitting* is that it guarantees stable approximations, simply by not allowing positive values of a_n .⁶

USAGE

Vector pole fitting is a valuable tool when working with electronics, partly because it is able to capture quickly shifting values over a frequency spectrum. Since (as described earlier) small changes to a circuit might have big implications, the plotted S-parameters may show just this very characteristic.

A disadvantage with this method is that it requires a lot of calculations. This is, however, often easily achieved with modern processors. It is, of course, entirely possible to write a program that performs these calculations, but in this project the version found in up to date versions of MATLAB was used.⁶

MEASUREMENT THEORY

INTRODUCTION

For readers unaccustomed to measurements on electronics, this section aims to cover the basic technology and terminology used in this thesis project.

OSCILLOSCOPES

An oscilloscope is the EKG equivalent of the electronics industry; it measures electrical signals and displays them on a screen. Since modern IC's electrical signals' fluctuation rate far exceeds those within a human heart, the oscilloscopes are usually equipped with functions that help the user to see the signals.

For repetitive signals; this can be done by plotting them on top of each other, effectively giving the user a real time view of the signal.

Since oscilloscopes are equipped with processors they may also act like computers, giving them the ability to do digital signal processing. This means that it is quite easy to get desired information from measured signals. One very commonly used feature within this industry is the *eye pattern*, which will be described later on.

Another feature that oscilloscopes are equipped with is a dynamic trigger system. It allows the user to specify what event (for instance; passing above a specified voltage level) that will trigger the oscilloscope to start recording.

As powerful as oscilloscopes' hardware have become, they are still subject to basic mathematical laws. The *Nyquist-Shannon sampling theorem* states that the sampling frequency (f_s) of a measurement must be at least twice that of the highest frequency component (f_0), as shown in (4.23)

$$f_s > \frac{f_0}{2} \quad (4.23)$$

This puts an effective limit on the performance of any oscilloscope. The equipment used in this thesis project was an oscilloscope from *Agilent Technologies' Infiniium 90000-X Series*, which is among the most powerful in the world. It is capable of measuring frequencies up to 32 GHz, and generally has a very low *noise floor* (a term describing how strong the signals need to be to distinguish them from background noise).

15, 31

NETWORK ANALYZERS

The difference between network analyzers and oscilloscopes is that oscilloscopes allow

the studying of specific signals, while network analyzers supply information of the entire system. What the network analyzer generates are the S-parameters of the system. The main advantage with network analyzers is that they are, usually, equipped with more than two ports; this gives them the ability to characterize large systems in a single measurement procedure. In this project different network analyzers were used depending on the situation; e.g. on what frequency spectrum that was necessary to obtain.

One last thing, that stands true for both oscilloscopes and network analyzers, is that they, in most cases, come equipped with software capable of de-embedding the test object from the cables. What this means will be described in a later section.³¹

EYE PATTERNS

One way to test the quality a propagated signal is to plot its *Eye pattern* (some literature may refer to them as *eye diagrams*). This is a standard procedure, and usually oscilloscopes are equipped with special functions to do this automatically.

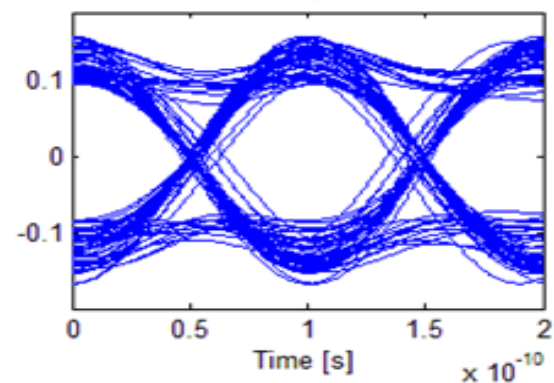


Figure 4.15. An example of an eye pattern measurement (the measurement was produced during the project).

Numerous important data can be obtained by an *eye pattern*; the rise and fall times of the

signal, the amplitude of “high” and “low” voltages, over/under-shoots and so on. A typical pattern may look like the one showed in figure 4.15.

The plot is generated when adding different parts of the *square waves* on top of each other. In the example above, every possible state of the signal is shown; transitions from high to low and vice versa, stationarity, and combinations of them both (e.g. a sequence [110]). Therefore it is possible to get a lot of information out of this small window.

The name’s reference to an *eye* is because of the middle section potential similarity to its geometric shape; if the rise/fall-times are increased the likeness becomes apparent.

Today’s modern measurement equipment can measure many of the parameters automatically and give more exact results, but sometimes it is possible to evaluate the state of the signal by simply looking at the pattern; the most obvious being if the *eye* becomes so small that it is impossible to tell the difference between high and low. If it is impossible for a human to tell the difference then it is also impossible for a machine, and that means the signal is so degraded that the information is lost.³⁵

EMBEDDING AND DE-EMBEDDING SIGNALS

INTRODUCTION

Let us assume that there is a system with the transfer function $H(s)$. It will also be assumed that a signal must pass through $G_1(s)$ to reach $H(s)$, and before it can be measured afterwards it must pass through $G_2(s)$. This means that the system, with transfer $H(s)$, is embedded between $G_1(s)$ and $G_2(s)$. If we wish to see the effect $H(s)$ alone has upon the signal we must then use the

following mathematical operation, shown in (4.24)

$$H(s) = G_2(s)^{-1}G_1(s)H(s)G_1(s)G_2(s)^{-1} \quad (4.24)$$

For analytical representations in s-domain, this is a very simple procedure. But if the ordinary functions get replaced by physical components it will get increasingly difficult to observe the desired system.

If one, for instance, wishes to know the S-parameters of a device and plans to derive them by the use of a network analyzer, then the cables connecting the analyzer to the *device under test* (often referred to as DUT) will impact the results. The DUT would have to be de-embedded from the cables in order to achieve the correct results.^{5, 13, 16}

T-PARAMETERS

T-parameters are closely related to the, previously described S-parameters. A problem with the S-parameter matrix (described in (4.20)) is that it cannot be used to combine structures, meaning that

$$\begin{bmatrix} S_{11} & S_{12} \\ S_{21} & S_{22} \end{bmatrix} \begin{bmatrix} S_{22} & S_{23} \\ S_{32} & S_{33} \end{bmatrix} \neq \begin{bmatrix} S_{11} & S_{13} \\ S_{31} & S_{33} \end{bmatrix}$$

This is where the T-parameters come into play. These parameters allows embedding and de-embedding by the use of simple matrix multiplication, since

$$T_1 \cdot T_2 = T_{21}$$

and

$$T_1^{-1} \cdot T_{21} = T_2$$

S-parameters can analytically be converted to T-parameters using (4.25)

$$\begin{bmatrix} T_{11} & T_{12} \\ T_{21} & T_{22} \end{bmatrix} = \begin{bmatrix} \frac{S_{11}S_{22}-S_{21}S_{12}}{S_{21}} & \frac{S_{11}}{S_{21}} \\ -\frac{S_{22}}{S_{21}} & \frac{1}{S_{21}} \end{bmatrix} \quad (4.25)$$

and vice versa by the use of (4.26)^{8,13}

$$\begin{bmatrix} S_{11} & S_{12} \\ S_{21} & S_{22} \end{bmatrix} = \begin{bmatrix} \frac{T_{12}}{T_{22}} & \frac{T_{11}T_{22} - T_{21}T_{12}}{T_{22}} \\ \frac{1}{T_{22}} & -\frac{T_{21}}{T_{22}} \end{bmatrix} \quad (4.26)$$

THE PROCEDURE

Now it is simply a problem of achieving accurate values for the S- or T-parameters that will be used to operate upon the embedded structure.

If the example earlier is revisited, this can be done either by simulating the cables (using advanced simulation software), simply guessing (e.g. assuming the same attenuation for every frequency) or by making measurements on the cables alone. After this, computers will be used to derive the de-embedded T-parameters and convert it back into S-parameters.

If everything was done correctly and the measurements perfectly captured the different characteristics, the same result as in (4.24) would have been achieved.

THE PROJECT

BACKGROUND

There are ways to measure signals within transmission line, and they usually involves probes. In the past this has worked quite well, but the rapid development of electronic technologies is making the method increasingly obsolete. The first, of two major reasons, for this is that a probe cannot be attached to an internal layer within the PCB and that results in the need to extend the circuit to one of the surface layers. This would result in the creation of a stub and also add the effect of the via to the measured signal. As was described earlier in this chapter, these effects get stronger as the frequencies increase.

The second major reason is that the load that a probe adds to a measurement point is capacitive, shown in figure 4.16.

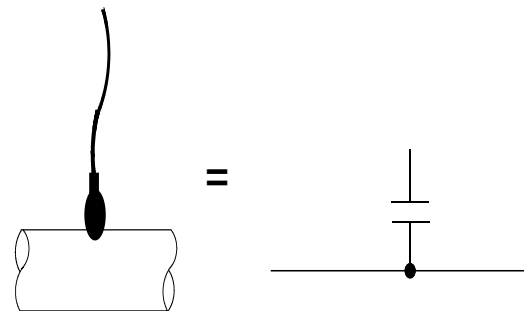


Figure 4.16. The load of a measurement probe upon a signal trace is capacitive, and therefore more influential on higher frequency signals.

A capacitance can act like a short circuit during brief moments of time, before it has become fully loaded. This means that a frequency, high enough, will make the probe destroy the internal signal propagation.

An exact point in the frequency spectrum, where this problem starts, does not exist. Instead the problems increase a little for each step, and more advanced technologies have now reached a point where traditional probing becomes too problematic.^{3,7}

PREVIOUS PROJECTS

Ericsson is not the only company that has encountered this problem and it is therefore reasonable to assume other similar projects may have been carried out, but that these have not been published. However, when doing research for this project I only encountered attempts to measure signals from the surface of PCBs or ICs, using different techniques.

It should be noted, though, that the literature studies for this project did not receive nearly enough time to completely rule out the possible existences of similar (or even identical) projects. Also, many projects have

had similar content as this but completely different goals (e.g. studying the crosstalk or modeling three dimensional structures with lumped components).^{14, 22, 23, 24, 25, 26, 27}

Still, the studies showed an increasing interest in *non contact* measurements within the scientific community, and if the reader is interested; he or she can, in the *References* chapter find several interesting papers on the subject.^{11, 12, 17, 18, 19, 20, 21, 28}

5. DESIGN INTRODUCTION

Before the *simulation* chapter is examined, it is recommended that the reader also studies this short chapter. Some necessary information is given, that will be helpful in the next chapter to get an overview of the simulation's part in the overall process.

SOME BASIC TERMINOLOGY

A conductor within a PCB may act like a *transmission line* and may therefore be referred to as such, another name is a *trace*. Within this thesis both names are used at different times and the reason is depending on the context. Also, if the goal is to clearly denote the difference between the different materials, then the traces may be referred to as the conductors. It is unfortunate if this brings confusion at times, but, while writing this report, it proved necessary to use all different notations.

A *measurement point* is a point in the PCB where the propagated signal is somehow measured. Regarding *non contact test points*, the point is actually more of a small volume. Still the notation *point* will be used in this thesis, as the overall volume of the PCB greatly exceeds that of the *measurement point*.

Two other important names are *source line* and *victim line*. They both describe parts in the constructed measurement point.

The *source line* is the trace in which the original signal is propagated, it is the source of the crosstalk, and the *victim line* is the trace in which the crosstalk is generated. To make the principle of *non contact test point* simple; in order to find out what the signal in the *source line* looks like, a *victim line* is placed next to it. In this *victim line* a voltage is induced, and it is later measured.

Sometimes the name *measurement structure* is also used. This refers to the entire structure that is used to measure the crosstalk.

GENERAL GOALS

Usually crosstalk is something that hardware developers try to avoid, but since this entire thesis is based on using it for measurements it was in this case vital that a lot was generated. An instruction, given by Ericsson, was that *non contact test points* would not be used upon signals weaker than 80mV. Another known criterion was that the oscilloscope, that would be used for the measurement, would be capable of measuring signals as weak as 0.6mVrms. This gave the requirement that the frequency domain value of the crosstalk was not allowed to be lower than $\frac{80mV}{0.6mV} = -42dB$

However, this was the theoretically lowest value and not a good goal. Additionally, the propagation path from the measurement point to the oscilloscope would contain a *via* and possibly other attenuating structures. Because of this, the goal was set to find a measurement structure, in which the transfer function (from *source line* to *victim line*) would reside above -20dB (within the desired frequency range). This goal was not a limit derived from theory, only a guessed estimate of what would actually be required and an additional safety margin.

There were simulations carried out, that included the *via* structure, but these will be excluded from the *simulation* chapter because of concerns regarding their accuracy. It was a general belief, at the department where this thesis work was done, that the simulation software yielded good approximations for crosstalk and same layer circuitry but was unreliable when simulating vias.

6. SIMULATION

In order to find the optimal geometry for the *measurement structure*, a huge amount of simulations were carried out. To begin with, these were done in HyperLynx (an advanced simulation software, from Mentor Graphics). There were a number of variables open to change, and in order to get an overview these were studied in a systematic fashion.

THE GENERAL SETUP

Several different designs were evaluated, but eventually the decision was made to create the two following the main candidates;

- A T-shaped measurement design, depicted in figure 6.1, that was to reside on the same layer as the source line (edge coupled).
- A T-shaped measurement design, depicted in figure 6.2, that was to reside on the layer above or below the source line (broadside coupled).

The reason why these two structures were chosen above the others will be explained later.

In figure 6.1 the changeable variables, mentioned previously, are also depicted. Note that D_0 is only open to change in the first structure. In the second the victim line is placed directly above or below the source line, and the distance between them was defined by the layer thickness. Of course, since the source line was part of a differential pair, there would actually be two measurement structures implemented on each test point. However, these would simply have mirrored structures.

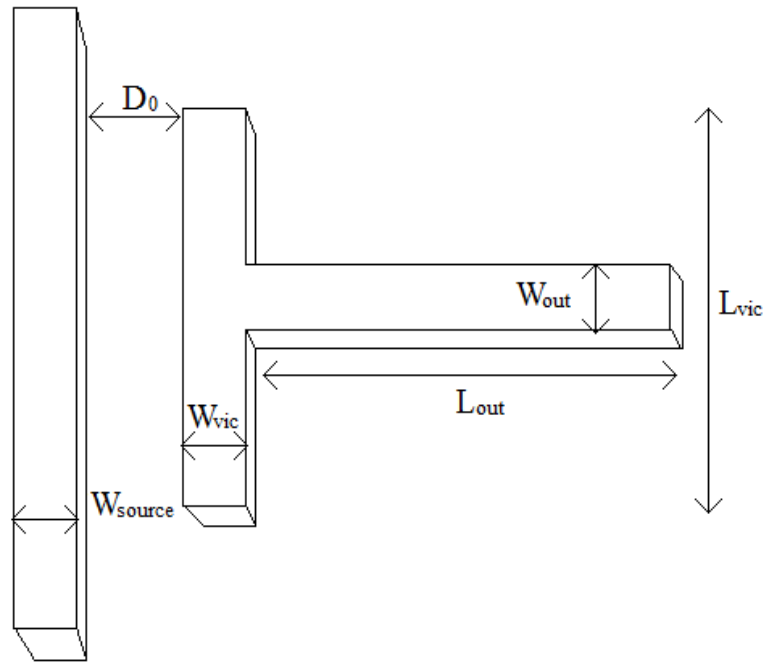


Figure 6.1. A schematic for the measurement design with parallel traces. The left trace constitutes the source line.

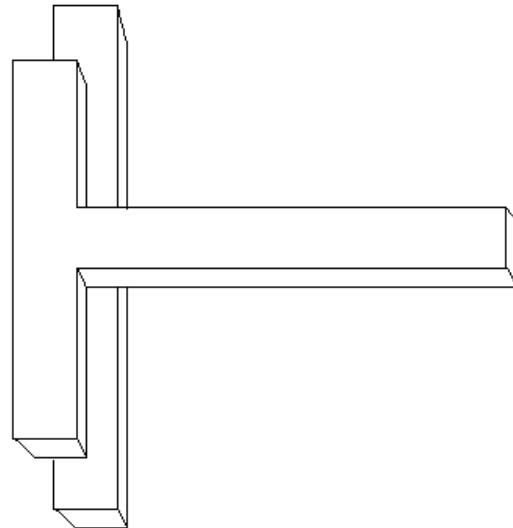


Figure 6.2. A schematic view for the design with the victim line place on another layer.

D_0 – DISTANCE BETWEEN THE TRACES

Unsurprisingly, the distance between the two conductors had a destructive effect on the crosstalk, and this effect increased with the distance. This effect is shown in figure 6.3, for a specific setup, but the effect was very general. No matter what the other variables were, the optimal distance was always the smallest possible.

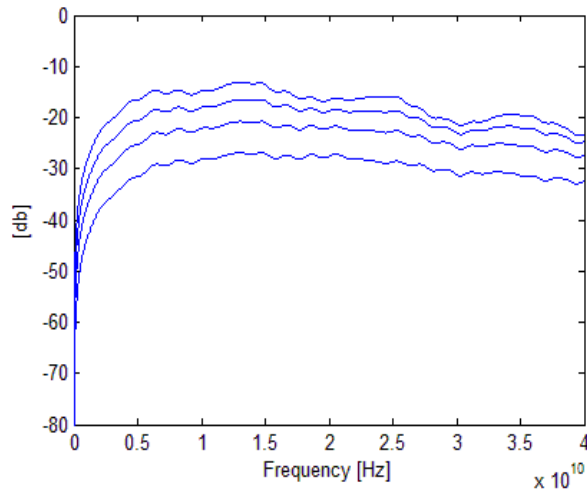


Figure 6.3. The simulated transfer functions, in frequency domain, for four different setups. All parameters are the same, except for the distance between the transmission lines. The distance is smallest in the upper line and then doubled for each new simulation.

Support for this conclusion is given in (6.1), a formula that was retrieved from the literature.

$$\text{Crosstalk} \approx \frac{K}{1 + \left(\frac{2D}{H}\right)^2} \quad (6.1)$$

where K is a constant that relates to the physical properties of the circuit, H is the distance to both the upper and the lower reference planes (in this approximation, these are assumed to be the same) and D is the distance between the center points of the transmission lines.

Hence, the distance D_0 should be kept to a minimum in order to maximize crosstalk. The design restriction on this matter, given by

Ericsson due to manufacturing constraints, was that the minimum possible distance between two traces is $100\mu\text{m}$.

L_{OUT} AND W_{OUT} – OUTPUT GEOMETRIES

This variable was necessary to include in order to see the attenuation of the captured signal as it propagated towards the measurement equipment. It should be noted that this transmission line still resides on the same layer as the others.

There were no special effects found when varying L_{out} , the signal was attenuated as much as expected, which can be related back to (4.10) and is shown in figure 6.4. Also related back to the theory section is the fact that the attenuation increases as the frequency of the signal goes up. Ideally L_{out} would be close to zero, but this would probably not be feasible in the actual design (because of construction limitations; the signal output would most likely not be placed right above or below the circuit).

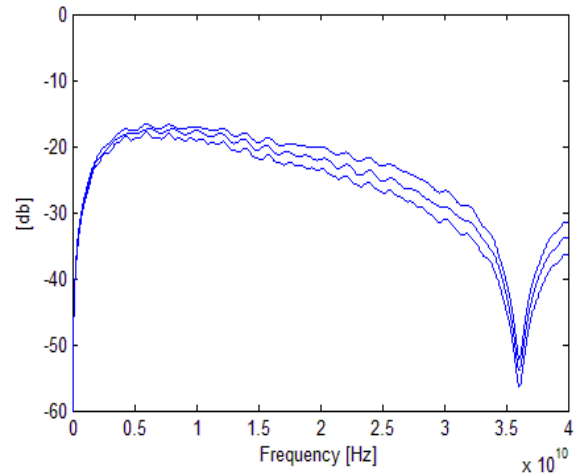


Figure 6.4. The effect of changing the length of L_{out} for a given setup. There is a difference between the three L_{out} values of approximately 4 cm.

Changing W_{out} did, however, have some interesting effects, as can be seen in figure 6.5. The output signal came to oscillate over the frequency spectra for simulations with certain W_{out} values.

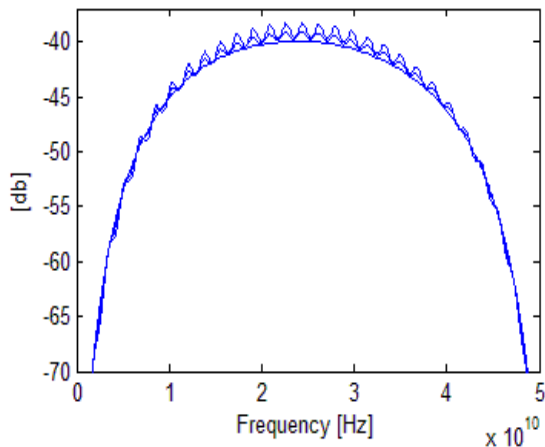


Figure 6.5. Three output signals plotted in frequency domain, as W_{out} was varied. In the smooth curve's simulation setup, W_{out} is equal to W_{vic} .

The reason for this is that changing the width of a transmission line will change its characteristic impedance, which in turn will cause frequency dependent reflection when connected to another transmission line (see (4.7)-(4.12)).

Though the simulations predicted that there would be some gain for certain frequencies, due to the mismatch, it also predicted that there would be some additional losses. It might look debatable whether to go with the smooth curve or the oscillating ones, but the decision was made to pick the one with the perfect match. This was because of distrust towards the simulations and an attempt to keep the number of uncertainties in the circuit's real behavior to a minimum.²⁹

W_{VIC} AND W_{SOURCE} – WIDTH DEPENDENCY

The results for W_{vic} and W_{source} came to vary a lot, depending on if the case with broadside coupled or edge coupled traces was simulated. To begin with, edge traces were simulated.

Varying W_{vic} and W_{source} showed the, a bit surprising, result that the width was optimal when it was as small as possible (for the design with parallel traces). Some results are

given figure 6.6 below. Like with D_0 , the conclusion was always the same, no matter what the other variables were: The wider the traces were, the less crosstalk was generated. This might sound strange, but if (6.1) is once again reviewed the explanation is clear. D relates not to the distance between the edges of the traces, but the distance between their center points. If the widths are increased, and D_0 maintained, then this distance is bound to increase. So once again, manufacturing constraints concluded the final design. Since $75\ \mu\text{m}$ was the smallest possible width for a trace, it was chosen.

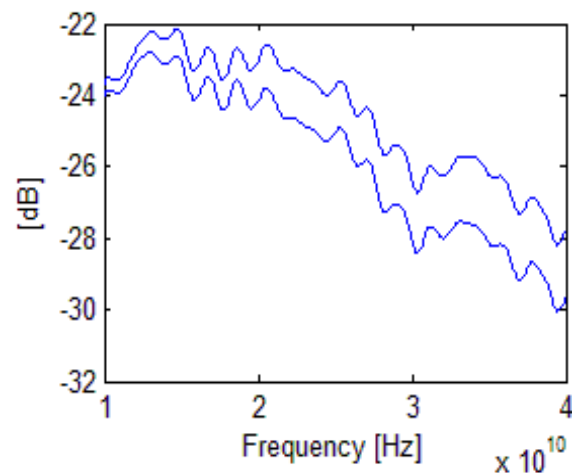


Figure 6.6. The difference in performance between two simulations when only W_{vic} and W_{source} are changed (in both simulations they have identical values). In the lower curve, W_{vic} and W_{source} bigger than in the other simulation.

Since (6.1) did not apply when the traces were placed on different layers, different results were expected for these cases. And just as expected, better results were generally achieved as the widths were increased, but not as much as one could think.

In figure 6.7 below, an example is given. Usually the maximum values along the frequency axis were not changed dramatically (sometimes even decreased) as the width increased. But the flanks tended to get sharper, resulting in increased gain for certain frequencies.

But the positive effects did eventually start to decline, there was not as much to gain from increasing the width from 120 μm to 140 μm as there was to increase it from 60 μm to 80 μm . In the end 120 μm became the width selected for the final test design.

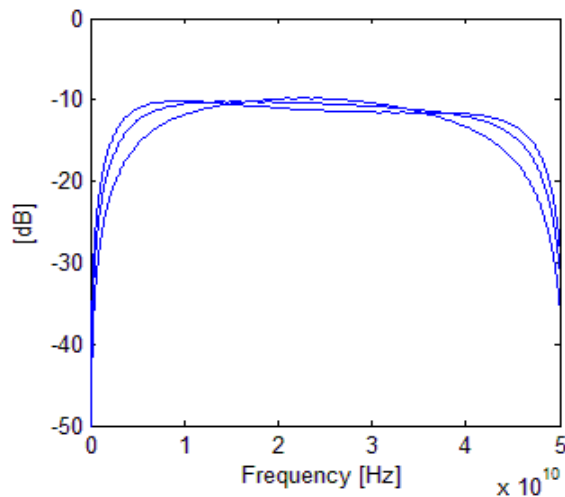


Figure 6.7. The difference between three W_{vic} 's and W_{source} 's for the design with the victim line placed vertically towards the source line (W_{vic} and W_{source} have identical values in every simulation). W_{vic} and W_{source} are bigger on the plots with sharper edges.

BROADSIDE OR EDGE COUPLED STRUCTURES

Without specifying certain parameters, it would be impossible to predict which of the alternatives that is superior. This is simply because they can be made identical if the geometries are chosen that way.

But given the production constraints ($D_0 \geq 100 \mu\text{m}$, and $75 \mu\text{m} \leq W_{vic}$ and $W_{source} \leq 120 \mu\text{m}$), and the fact that the distance between the layers was predefined, it was clearly two distinctly different alternatives.

In every simulation the structure with parallel lines was outperformed. Consistently, it proved better to place the *victim line* above or below the *source line*. An example of this is given in figure 6.8. Usually the difference in result was between 10 dB and 15 dB.

To derive these results from science is not an easy task, and a complete explanation would require extensive calculations using electromagnetic field theory and solid state physics, but it is possible to make a quicker estimation.

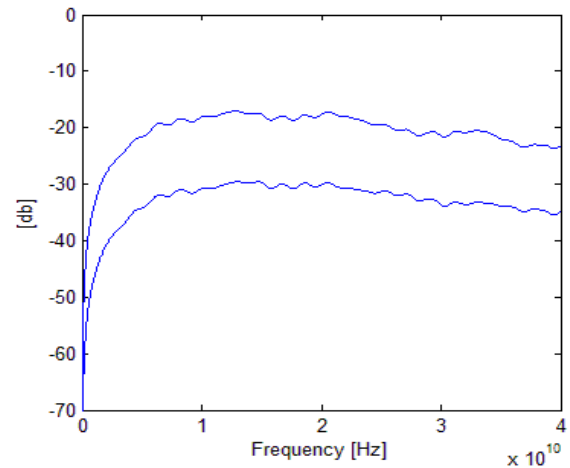


Figure 6.8 A typical difference in performance between a construction with traces placed vertically (upper line) to each other and in parallel (lower line).

If the inductive coupling is studied, then the case with a T-shaped measurement structure will present a very special situation; the inductive coupling will be cancelled out by itself. The reason for this is that the magnetic field (that constitutes the inductive coupling), will direct a number of positive and negative charges (in reality; the positive charges are a deficit of electrons) in different directions. But, in theory, the numbers of both kinds are the same. This means that those that get reflected backwards, towards the middle and the output of the measurement structure, will cancel each other out. Since this effect requires identical travel distances for the charges, the effect is only present for symmetric T-shaped structures. In reality, it is not likely that a T-shaped structure would be perfectly immune to the effects of inductive coupling, but since the simulations were based on theory, this explanation is used. It is thus assumed that the difference in

capacitive coupling is responsible for most of the difference in performance. Since the capacitive coupling can be modeled as a capacitance, the next step is to compare the capacitances for the different options.

Since the current (I_1 , see theory section) generated by the coupling is proportional to the capacitance between the two lines, according to (6.2) below, the generated voltage will also be proportional.

$$I = C \frac{dV}{dt} \quad (6.2)$$

If the parallel plate approximation (6.3) is used (A equals area), it is apparent that the capacitive coupling ratio between the two cases is equal to (6.4). Let A_1 be the height of the *victim line* ($18\mu\text{m}$) times its length and A_2 be the width of the *source line* ($75\mu\text{m}$) times the length it follows the *victim line*.

$$C = \frac{\epsilon_0 \epsilon_r A}{d} \quad (6.3)$$

$$\begin{aligned} \frac{A_1}{A_2} &= \frac{L_{vic} \cdot H_{vic}}{L_{source} \cdot W_{source}} \\ &= \frac{18\mu\text{m}}{75\mu\text{m}} \\ &= 0.24 = -12.4\text{dB} \end{aligned} \quad (6.4)$$

This is not a perfect approximation, since the conductors are assumed to be thin and flat. But since the length of the conductors (even for the case with parallel lines) greatly exceeds any other geometric property, there will be some truth to the approximation. And the approximated difference complies very well with the simulated ones. It should be mentioned that all the values used in (6.4) were also used in the simulations, shown in figure 6.8.

Judging from these results, the structure of choice would be the broadside coupled structure. But there were concerns about this, once again due to manufacturing constraints.

When placing a trace above another, there is a possibility that the distance between them will vary along their lengths. This would cause unpredictable behavior, which in turn could render the signal reconstruction software invalid.

Because of this, the decision was made to build in both alternatives in the test PCB and evaluate later which one that performed the best.

L_{vic} – LENGTH OF THE VICTIM LINE

L_{vic} proved to be the most difficult value to optimize and this was mostly due to, what at first seemed like, an unpredictable behavior.

It was partly because of the assumption that an increased L_{vic} would always give an increased gain for the crosstalk, which, as can be seen in figure 6.9 below, was not a general rule.

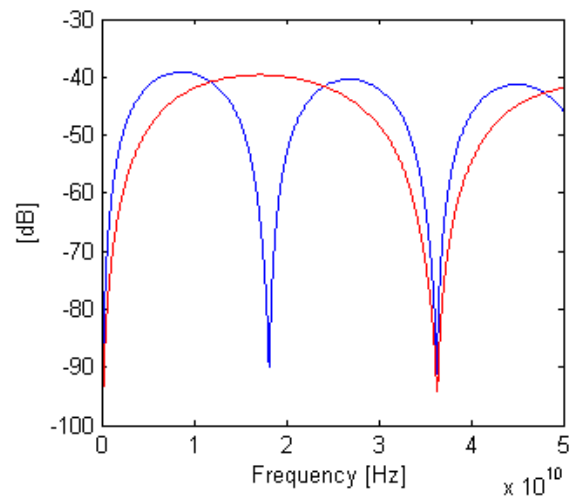


Figure 6.9. The crosstalk, of two different simulations, in frequency domain. The difference between the simulations was that the L_{vic} relating to the blue curve was twice as long as the L_{vic} relating to the red curve.

The question quickly arises; why does a longer L_{vic} not automatically generate a larger gain? The following assumptions were made to answer that question:

It may be tempting to believe that two transmission lines would generate more crosstalk, the longer they are. But as the simulation has shown, this is not the case. In order to explain this peculiar result, we will study the crosstalk generated by a single, arbitrary frequency (f_0).

Consider the situation in figure 6.10. Assume that the x -axis for the upper graph is the *source line*, and that the other x -axis is the *victim line*.

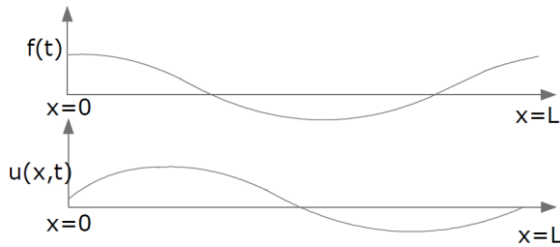


Figure 6.10. A schematic of the relation between the sinusoidal voltage in the source line and the induced voltage in the victim line. The x -axis of the upper graphs symbolizes the source line.

Let us assume that the signal that enters the upper transmission line at $x=0$ is described by (6.5) below

$$f(t) = A \sin(2\pi f_0 t + \theta_1) \quad (6.5)$$

We cannot know directly what the generated crosstalk looks like, but we will do two assumptions here. First of all: The crosstalk generated at any point, x_0 , in the second line is generated by the voltage in x_0 at the upper line. Secondly: the generated crosstalk is proportional to the derivate of the voltage in the upper line. Now we have enough information to describe $u(x,t)$ in (6.6) below (B equals A times other constants).

$$\begin{aligned} u(x,t) &= B f' \left(t - \frac{x}{c_0} \right) \\ &= 2\pi B f_0 \cos \left(2\pi f_0 \left(t - \frac{x}{c_0} \right) + \theta_1 \right) \quad (6.6) \end{aligned}$$

$$\begin{aligned} &= [2\pi f_0 t + \theta_1 = -\theta_2(t) \cos(-x) = \cos(x)] \\ &= 2\pi B f_0 \cos \left(\frac{2\pi f_0 x}{c_0} + \theta_2(t) \right) \end{aligned}$$

This is a complete description of the voltage that is being generated by the crosstalk at point x at time t . The next step is to integrate the amplitude from $x=0$ to $x=L$.

$$\begin{aligned} &\int_0^L u(x,t) dx = \\ &= \frac{2\pi f_0}{2\pi f_0} B c_0 \left[\sin \left(\frac{2\pi f_0 x}{c_0} + \theta_2(t) \right) \right]_{x=0}^L = \\ &= -B c_0 \left(\sin(\theta_2(t)) - \sin \left(\frac{2\pi f_0 L}{c_0} + \theta_2(t) \right) \right) \\ &= \left[\frac{f_0}{c_0} = \frac{1}{\lambda_0} \right] = \\ &= \left[\sin(a) - \sin(b) = 2 \cos \left(\frac{a+b}{2} \right) \sin \left(\frac{a-b}{2} \right) \right] \\ &= -2B c_0 \left(\cos \left(\frac{\pi L}{\lambda} + \theta_2(t) \right) \sin \left(\frac{\pi L}{\lambda} \right) \right) \end{aligned}$$

This effectively proves that it is not a guarantee to get better crosstalk, simply by increasing the length. The derivation only applies to sinusoidal functions in the *source line*, but as described in the *Theory* chapter; almost any time dependent function can be seen as the sum of different sinusoidal functions. It is therefore also important to observe the frequency content of the signal in the source line, and tailor L_{vic} accordingly.

However, this theory will not give a complete description of the frequency responses when varying L_{vic} . In figure 6.11, the frequency response for a T-shaped measurement structure is shown, where the ordinary x -axis is replaced by L_{vic} 's relation to the wavelength. It is important to note that the sides of the T-structure have different lengths in this example, and the reason for this distinction will be explained later.

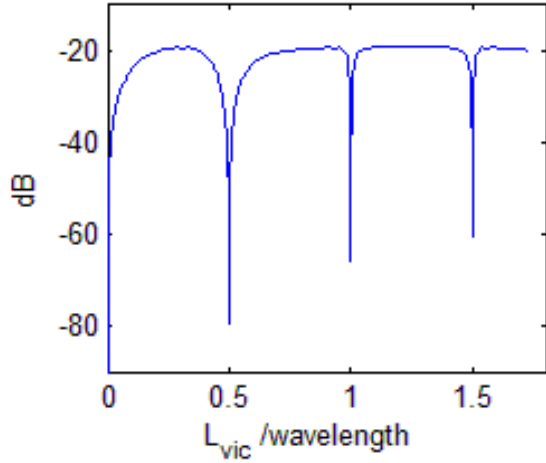


Figure 6.11. The simulated crosstalk for an uneven T-shaped measurement structure, plotted against the ratio between L_{vic} and the wavelength.

As can be seen in the figure, the values of the transfer function along the x-axis crashes at every multiple of 0.5, and this is twice as often as predicted earlier. That points to the conclusion that there is some other kind of effect present, that the previous analytical approach could not predict. The new effect makes the crosstalk proportional to $\sin(\frac{2\pi L}{\lambda})$.

It is likely that this effect is the result of some kind of reflection that may be hard to see directly, but there was one other effect that could cancel the unexplained part out; if the arms of the T were made equally long, then these dips were only present at the frequencies predicted earlier. It therefore proved advantageous to use the structure with a symmetric T, and choose the length of L_{vic} so that the desired frequencies are targeted. If desired, (6.7) may be used to predict where the frequency dips will show up for a symmetric T-structure. For an unsymmetrical design, (6.8) may be used.

$$\frac{c}{2\sqrt{\epsilon_r} \cdot L_{vic}} \quad (6.7)$$

$$\frac{c}{\sqrt{\epsilon_r} \cdot L_{vic}} \quad (6.8)$$

In the case for this thesis work, L_{vic} was chosen as 12 mm. This would place the first dip at about 12 GHz. Also, for evaluating the frequencies of 26Gbit/s, the length of 2.8 mm was selected (placing the first dip at about 50 GHz). The crosstalk for these two structures is shown in figure 6.12.

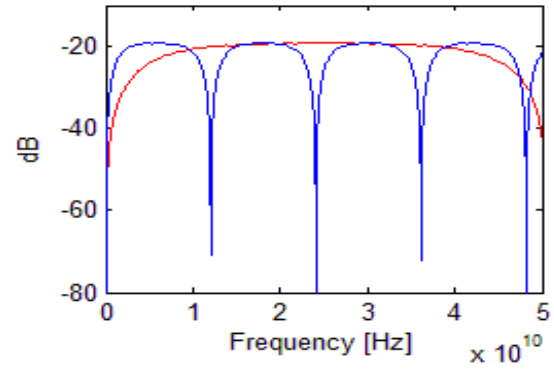


Figure 6.12. A comparison of the crosstalk between the L_{vic} selected for 10Gbit/s (blue) and 26 Gbit/s (red).

Note that measurement structures capable of catching higher frequencies can be shorter, but the downside is that they will not be able to see the lower frequencies as well as higher ones.

VERIFICATION OF THE HYPERLYNX SIMULATIONS

Promising simulation results were obtained in *HyperLynx*, but in order to verify them a different simulation software was used. A big problem with *HyperLynx* is that coupling effects can only be simulated between parallel traces, the effect being that the rest of the geometries will not make a difference. The problem it generated for this project is shown in figure 6.13.

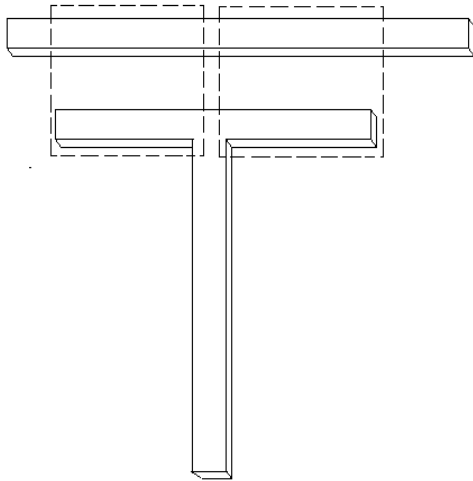


Figure 6.13. When the structure above was simulated in HyperLynx, the coupling effects were isolated to separate regions. In the picture, two such regions are marked, but the coupling effects are completely independent of the space outside these regions.

In order to test these results, there was a need for a software that would simulate the coupling effects of the entire structure at once (in figure 6.13, this would be equivalent to removing one square, and expanding the other until it becomes a frame for the entire figure). The program of choice was *Simbeor2011* by *Simberian Inc.* The same frequency span was simulated (from 0 to 50GHz), and a comparison can be seen in figure 6.14 below.

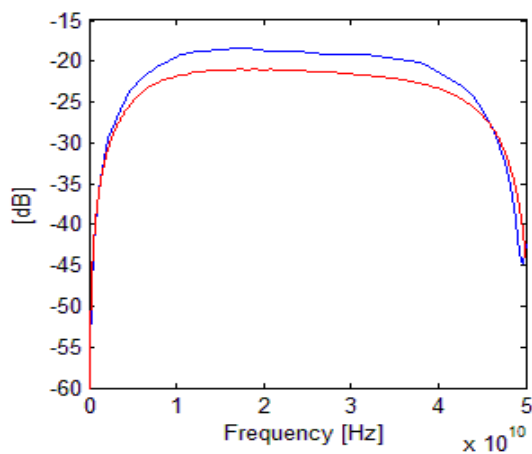


Figure 6.14. The generated crosstalk (of the structure in figure 6.13), over a frequency span. A

comparison is shown between the results from HyperLynx (red line) and Simbeor2011 (blue line).

As can be seen, the general behaviors of the curves were the same, and the crosstalk predicted by *Simbeor2011* did actually exceed that predicted by *HyperLynx*. Since the only difference was slightly better results, the comparison yielded an increased trust in the chosen design.

For full disclosure it should be mentioned that another simulation software was used before *Simbeor2011*, and that was *Advanced Design System (ADS)* by *Agilent*. It did give results that were fairly consistent with *HyperLynx*, as long as the conducting material was approximated as perfectly conducting (infinite conductivity). When, instead, copper was selected, the generated results started to look very strange and questionable (fluctuating heavily, and reaching peak levels far above any generated earlier). The reason for these strange results is not entirely clear; it could be a bug in the system, but it could also be lack of experience with the software (it had not been used previously at the department, so there was no in house support available). Since more credible results had been obtained simply by using *Simbeor2011*, the matter was deemed concluded and the problem not investigated further.

OTHER STRUCTURES

THE L-SHAPED STRUCTURE

There were also numerous simulations made with different measurement structures, mostly the L-shaped one. As the name suggests, the *source line* was shaped like an L instead of a T. This structure is shown in figure 6.15.

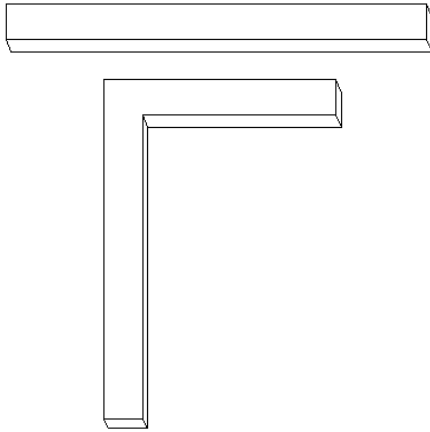


Figure 6.15. *The L-shaped measurement structure.*

Obviously, these were among the first simulations to be made during this thesis work and it aimed at comparing the results between the T-shape and the L-shape. Generally, T-shaped structures outperformed L-shaped ones. The difference can be seen in figure 6.16. In that figure, it is clear that both structures reach similar peak values, but that the T-shape yields significantly better results for almost all other frequencies. This is a typical result when comparing the two structures, as long as they are adapted for the same target frequencies. However, there is one major advantage with the L-shape; it requires only half the space compared to the T-shape. That means that it is possible to target a specific frequency interval with only half the space, but with reduced performance. This would, however, make the shape ideal if the wish is to measure a single frequency or a very limited frequency spectrum.

The other geometric parameters (apart for L_{vic}), previously described for the T-shaped structure, could of course also be changed for the L-shape, but the effects of changes proved very similar between the structures.

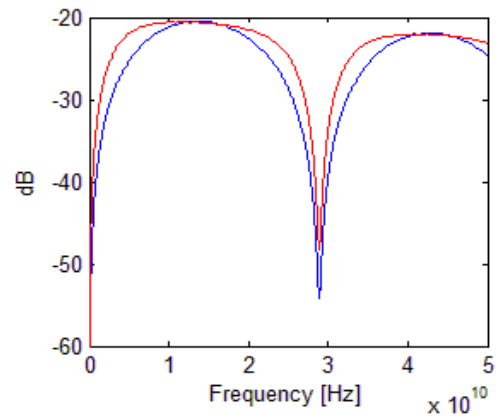


Figure 6.16. *A typical comparison in performance between the T-shaped (red) and the L-shaped (blue) structures.*

Since this structure was always outperformed, most other simulations came to be done with the T-structure. However, enough simulations were made to conclude that the difference in performance was very general, and the decision was made to implement it in the physical design for evaluation. Still, T-shaped structures were to remain the basis for this project.

7. IMPLEMENTATION

INTRODUCTION

When the simulation process was finished, the next step was to implement the designs on an actual PCB. The idea was the following: there was a board upon which several signals behaved unexpectedly, and non contact test points would be applied to some of these signals in hope of finding an explanation. Upon this board some extra test points would also be implemented, but they would only be for experimental purposes. For these additional test points, extra inputs and transmission lines were added to enable direct control of the source lines.

In the rest of this thesis, the test points applied upon original transmission lines will be referred to as the *applied test points* and the ones where extra source lines have been added as the *experimental test points*.

Though the plan was to later implement test points like this upon mass produced boards, only two would be manufactured for this project, one with surface mounted devices and one without them.

CHOSEN DESIGNS

APPLIED TEST POINTS

For the *applied test points* the ordinary T-shaped structure was to be implemented and also a rectangle shaped structure. If it were to prove possible, the two would be applied on the same source lines to simplify comparison.

The rectangle shaped structure was a design that was somewhat of an experiment. It is depicted in figure 7.1, and the idea behind it was to capture undesired common mode signals.

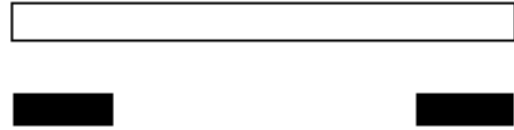


Figure 7.1. The cross section of the test point with a rectangle shaped victim line (white) and a source line (black) in differential mode.

If the signals in the two conductors are in differential mode they generate the crosstalk S_1 and S_2 ($S_2 = -S_1$) in the victim line. If the differential pair is also subjected to a disturbance that adds the same voltage on both lines, then the crosstalk induced in the victim line will be

$$(S_1 + S_3) + (S_2 + S_3) = 2S_3$$

This would in theory give direct measurement capabilities of the added common mode signal. The simulations in the previous chapter had shown that a measurement structure, on an adjacent layer, picks up the optimal amount of crosstalk if its outer borders coincide with those of the source lines. Because of this, the width of these *applied test points* was determined by the geometries of the existing layout.

As for the T-shaped measurement structure, the length had already been determined by simulations, and both the broad side coupled and the edge coupled designs were to be implemented.

EXPERIMENTAL TEST POINTS

Since the *experimental test points* were not subjected to constraints regarding their location, they would be easier to implement. But, since the source lines would also need to be added, there would be two additional pairs of inputs/outputs. The designs that were to be implemented as experimental test points were the following:

- 4 T-shaped measurement structures: one pair tailored for 10Gbit/s and one for 26Gbit/s. Each pair was to have one broadside coupled structure and edge coupled structure.
- 2 L-shaped measurement structures, designed for 10Gbit/s, one in parallel and one on a different layer as the source line.
- 2 different rectangle-shaped structures: one designed for 10Gbit/s and one for 26Gbit/s.
- 1 structure with only two source lines with the same lengths but with very different propagation paths.

Since the T-shaped structure yielded the best results during the simulation process, it became the main source of interest. Therefore it was granted 4 experimental test points.

The L-shaped measurement structure was mostly included to evaluate whether the simulations gave correct results.

The rectangle shaped structures were put in to evaluate performance for both 10Gbit/s and 26Gbit/s.

Finally, the 2 source lines were included to study what effect the propagation path would have upon a signal. One of the source lines had a very straight path, while the other travelled with many curves (its constant turning often resulted in potential crosstalk with itself).

INPUT/OUTPUT

Because of the lack of free space on the bottom and surface layers, two different input/outputs were implemented. One was the so called SMP connector and the other was called a SMA connector. SMP connectors are outputs/inputs that require a surface mounted attachment, on either of the surface layers. It gives an excellent stability to the structure, but unfortunately it requires a lot of additional space. The decision was made to use SMP's

for the *applied test points*, since they were also expected to lower the noise floor.

A description of the SMP connector can be found in figure 7.2. The reason that *vias* are necessary to implement also is that they will carry the return current (as described in the *Theory* chapter; there is always a current going in the opposite direction).

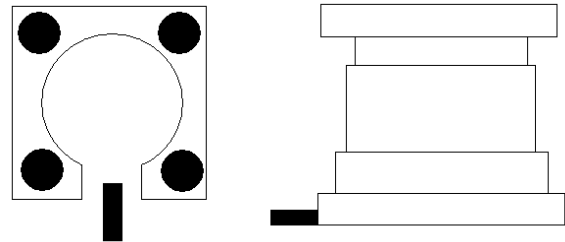


Figure 7.2. A description of a SMP connector; the left pictures show the PCB's surface layers structure (the square being a copper surface, the black circles are ground vias and the black rectangle is the input/output), while the right part of the figure shows the SMP connector from the side (the black rectangle of the right figure is placed upon the black rectangle of the left one).

For the *experimental test point* SMA cable connectors were to be used. Their main advantage was that that it required less space on the circuit board, making placement easier. The reason for this was that they were mounted at the end of a coaxial cable. The structure of SMA cable connectors is shown in figure 7.3 below, and once again *vias* surround the main conductor.

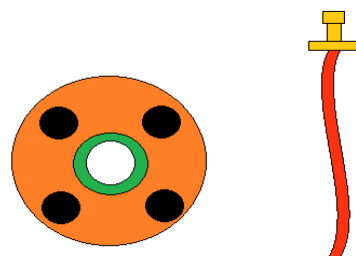


Figure 7.3. A description of a SMA cable connection. The left figure is the layout on the PCB (black holes are grounded vias, the orange color is

copper, the green is isolated materials and the white hole is where the cable enters the PCB), while the left figure shows the entire coaxial cable structure.

Since the source lines of these test points were to be directly controlled it would not be necessary to strive for such a low noise floor. Still, it would hopefully be enough to capture the S-parameters of the structure.

TEST VIAS

A general concern during the simulation phase of this thesis was that it is hard to accurately simulate a *via*. This is very problematic, since the effect that vias have upon higher frequency signals is huge. In an attempt to observe the actual effect that the *vias* would have, some test vias were also implemented. *Ericsson* was able to provide a MATLAB based software, capable of calculating the transfer function of a *via* if given the necessary information.

This necessary information was two sets of S-parameters, for the two structures depicted in figure 7.4. The requirements were that L_{12} would be equal to L_{21} , and that L_{11} would be significantly longer than L_{22} (L_{22} could very well be just a couple millimeters, while L_{11} had to be more than 50 mm). If this was implemented correctly, and the S-parameters fed to the software, you would hopefully receive the combined S-parameters for L_{12} , the *via* and half of L_{22} (i.e. half of the second structure in figure 7.4).

In the ideal case the lines would be perfectly straight in the layout as well, but this proved unfeasible in the layout. Still they were made as straight as possible, and L_{12} and L_{21} were always given the exact same geometric shapes.

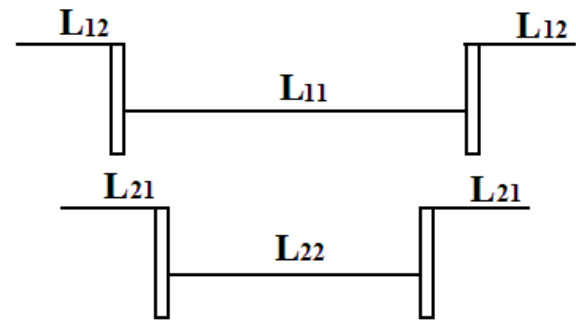


Figure 7.4. The schematic setups for via test. The horizontal lines symbolize simple conductors and the rectangles are vias. Apart from the length difference between L_{11} and L_{22} , the setups are identical.

Two of these test setups were implemented, one for SMP and another for SMA. Obviously L_{12} and L_{21} were equal to zero for the SMA's test setup.

CAD (COMPUTER AIDED DESIGN)

In today's industry, CAD has become a very important tool, close to invaluable in many areas. It replaces the traditional hand drawn blueprints and enables quick changes and updates. Another advantage is the possibility to design CAD software that also performs simulations, effectively testing what the blueprints will generate in reality. A simple example of CAD software (though not often thought of as such) is *Microsoft Word*; it allows the user to build easily changeable blueprints of the documents before printing, and also offers other helpful features.

For PCB design, *Ericsson* uses software from *Cadence Design Systems* that has been modified to better suit the specific needs of the company. There are two stages in the design process for a circuit board; drawing the schematic and creating the layout. Thanks to CAD, these two processes are now tightly tied together.³⁰

SCHEMATIC DESIGN

The software used at this stage is called *BPC* (Board Platform Cadence) and is the result of a cooperation between *Ericsson* and *Cadence Inc.*

It enables the user to make connections between different components, without specifying any geometry. For instance, a connection between two capacitors may look long on the schematic, but on the actual design be just a couple of microns. All that the schematic had defined in this case was that the capacitors were connected.

It is however possible (and very common) to add *constraints* to the schematic, defining maximum and minimum properties. A simple example is to define a minimum distance between two conductors, to decrease the risk of crosstalk. These constraints could be made very general or very specific, and they become extremely important in later stages of the design.

One important thing about *BPC* is that instead of adding a general component (e.g. a resistor) and defining its properties, the user adds a specific component from the database with predefined characteristics. This simplifies the manufacturing of the board tremendously, since there never will be any doubt of what component that best matches the criteria.

There are of course additional features in this software, but very few were used during this project. This was because the circuits were implemented in a finished design, and the amount of actual added transmission lines was quite small. Also, no additional simulations were necessary.

Once the schematic is complete, it is packaged into another file type and archived, later to be retrieved during the layout process.

LAYOUT PROCESS

The important difference between the look of the schematic and the layout is, of course, that in the layout, what you see is what you get. If one distance looks twice another distance, then it will also be like that in reality. The software used during this process was called *Allegro PCB Design* and, as mentioned before, it was a *Cadence* product.

Since the process required adding circuitry to a completed board, it directly posted the challenge of allocating the necessary space. For obvious reason (both legal and practical) the complete layout cannot be shown in this report, but it is sufficient to say that the process of implementing the design was very time consuming. In the end, some concessions had to be made in order to implement it all. Unfortunately they often meant jeopardizing the signal integrity by adding *vias* close to the test point or removing the *vias* that would channel some of the *return currents*. However, it was always done in a way that would minimize the effects upon the actual measurements.

ENCOUNTERED PROBLEMS

There are numerous obstacles when adding circuitry to an already finished design, the first one is of course the lack of free space. This problem was worse for the *applied test points* since the source lines, which they were to target, had almost fixed paths. It was possible to make some small changes to the paths, moving it a little, but the layer and the general area of its path were fixed.

This resulted in the need to bend the structures. For instance, to achieve the correct length of the test points, structures like the one in figure 7.5 needed to be implemented. The problematic thing about this structure was that it was difficult to test by simulating.

HyperLynx did not support testing of these structures, due to reasons described in *Verification of the HyperLynx simulations*. It would be possible to use some different software, and once again model it by three dimensions, but this would require time that simply was not available. The choice was made to keep these structures, and hope that it would not heavily affect the results. This problem was encountered for both types of *applied test points*, but not for the *experimental ones*.

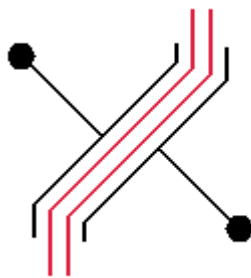


Figure 7.5. A schematic example of how the applied test points (depicted black) needed to be bent in order to follow the differential pair of source lines (red).

Another constantly occurring problem was to maintain the signal integrity of the victim lines. Since the signals induced in the test points were to be quite low, other small disturbances could have a significant impact. This was extra problematic on layers that were close to a power plane, the reason being that fluctuations in these planes easily could induce voltages into the test circuits. The solution to this problem was often to make small holes in the power planes, so that the test structure would not be close to it.

Other sources of disturbances, such as vias and other transmission lines were usually quite simple to move away from the circuit.

8. SIGNAL PROCESSING

INTRODUCTION AND GOALS

The goal of the signal processing was of course to use voltages induced in the *victim line* to recreate the information of the *source line* as accurately as possible. However, to what extent that would be possible was a, in advance, difficult question to answer. It was to depend on; how accurate the simulations were, the amount of disturbances within the PCB, the precision of manufacture and much more. All of these reasons combined gave a great uncertainty to the process.

Still some signal processing software would be produced and the idea was to implement it in an oscilloscope, so that the processing could be done directly. The practical applications will be more thoroughly described in later chapters, instead the principle of the programming will be explained here.

THEORETICAL APPROACHES

S-PARAMETERS

There are three ways to obtain the S-parameters of a circuit; analytically calculating them, simulating them or measuring them. One alternative was directly rejected; to analytically calculate the S-parameters of a high frequency circuit was not an alternative. The reason being the complexity of such calculations (see *Theory*).

In this part of the report it is not important how the S-parameters are obtained, as long as they can be considered fairly accurate. For they were to be used as the transfer functions they are. If each value for the S-parameters (S_{orig}) is inverted, according to (8.1), then the frequency domain representation (S_{inv}) from the victim line to the source line is obtained.

$$S_{inv}(f) = \frac{1}{S_{orig}(f)} \quad (8.1)$$

If preciously accurate, this would be enough information to recreate the original signal almost perfectly. The reason that it is only “almost” is that since the S_{orig} may contain zeroes, some information will be irretrievably lost. Unfortunately, this was definitely going to be the case since DC would not generate any crosstalk, and therefore the correct transfer function value for S_{orig} would be equal to zero. Also, the values close to 0 Hz were going to be so low that the accuracy for S_{inv} could rightfully be questioned for them.

VECTOR POLE FITTING

The original idea was to approximate $S_{inv}(f)$ by *vector pole fitting*. If this was achieved, then $S_{inv}(f)$ could simply be convolved with the measured signal to recreate the original one. But this approach did not succeed.

When modeling $S_{inv}(f)$ with *Rationalfit* (MATLAB’s function for utilizing *vector pole fitting*), quite poor values were generally achieved for the frequency span defined by simulations (0-50 GHz). A comparison can be seen in figure 8.1.

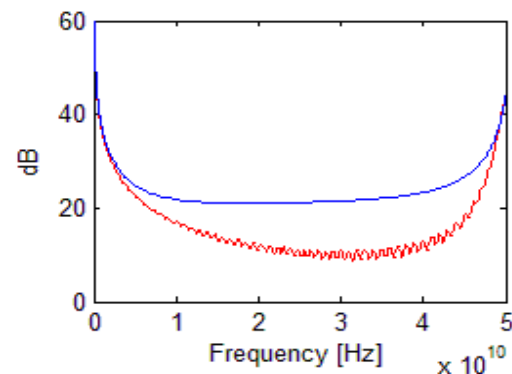


Figure 8.1. The S_{inv} (blue) achieved by inverting the simulated results of S_{orig} and the fitted approximation (red).

Still, in order to test this fitted transfer function, simulations were carried out in

HyperLynx. These simulations gave an estimate of what the real signal (captured by the *victim line*) would look like. The simulated measurements were then used to test whether there was any validity to the transfer function. Unfortunately, the results achieved were far from satisfactory. An example can be seen in figure 8.2.

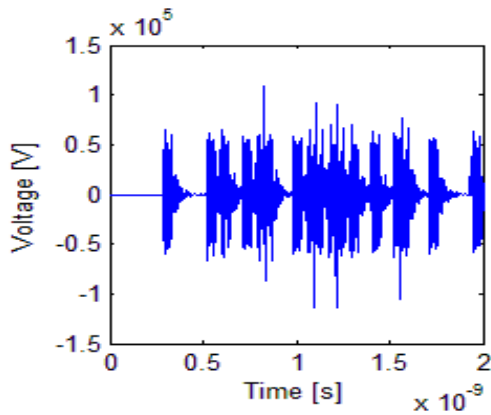


Figure 8.2. $h_{source}(t)$, calculated by the vector pole fitting approach. The reader should notice the scale on the y-axis.

The explanation for these unfavorable results can be seen in figure 8.3, where the frequency response for the fitted transfer function is shown, but this time over a wider frequency spectrum.

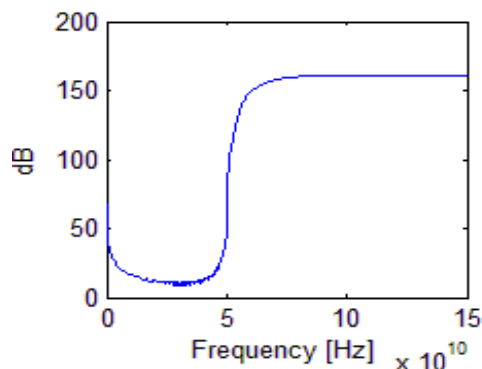


Figure 8.3. The vector fitted approximation, with a wider spectrum.

Obviously the fitted transfer function was practically unstable and, though several attempts were made, this defect was not corrected. No conclusive explanation as to

why this happened could be found. It should be noted that simple changes to the S-parameters were made in advance to avoid singularities, like the one described earlier. Still, this did not help. Eventually, the approach with *vector pole fitting* had to be abandoned.

FOURIER SERIES ANALYSIS

Instead *Fourier series analysis* was to be used. The approach this time differed from the previous one in the following way; instead of approximating a transfer function of the S-parameters, an estimate of the frequency content of the measured signals was made.

It all worked like this: If the signal in the *source line* is denoted $h_{source}(t)$ and the resulting signal in the *victim line* is called $h_{vic}(t)$ (the frequency representations of them are $H_{source}(f)$ and $H_{vic}(f)$), then the following relation (8.2) holds

$$H_{vic}(f) \cdot S_{inv}(f) = H_{source}(f) \quad (8.2)$$

Since both $H_{vic}(f)$ and $S_{inv}(f)$ are known, it is possible to calculate $H_{source}(f)$ by simple scalar multiplication. If $H_{source}(f)$ is then transformed back into the time domain (see (8.3) below) the desired results would be achieved.

$$\int_{-\infty}^{\infty} H_{source}(f) \cdot e^{i\omega t} df = h_{source}(t) \quad (8.3)$$

The same kind of test was done for this approach as for the last one. Since $H_{vic}(f)$ is simply a complex valued vector it was not necessary to check for stability outside of the specified frequency spectrum, but singularities were of course removed beforehand.

This method did not only perform acceptable in the tests, it performed really well. A demonstration of the accuracy can be seen in figure 8.4. The figure also demonstrates a

problem: since DC does not generate any crosstalk, it will be impossible to calculate the offset.

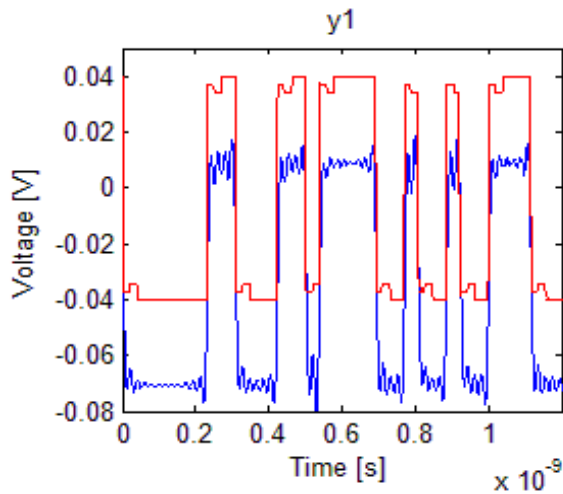


Figure 8.4. A comparison between the simulated $h_{source}(t)$ (red) and the one calculated by Fourier series analyzes (blue) using the simulated $h_{vic}(t)$.

However, even beforehand it was obvious that this method would bring some difficulties; apart from its sensitivity to noise (a fault that it would share with any other method) it would require much computer processing. If the signal that one wished to analyze was long, then enormous amounts of calculations would be required to fulfill the task.

The solution to this problem was to divide the measured signal into smaller segments, and analyze each of them separately. This would effectively decrease the computation time, but in turn generate another problem. As could be seen in figure 8.4 earlier, the offset became unpredictable, and it also varied between the different segments. To counteract that, an algorithm that calculated the difference between top and bottom values and used them to guess the offset was created. This also meant that the segments needed to be large enough so that both 0's and 1's were likely to be represented.

TESTING THE PRINCIPLE

BACKGROUND

Once the layout of a PCB is finished, there is some waiting time before the manufacturing process and the deliveries are completed. For this project it took about two weeks until the first boards were obtained. During this time, tests were carried out on a different board in order to evaluate the principle of *non contact test points*.

This board was an older design, built to test SMP connectors (the same one that was used in this project) and the amount of crosstalk conductors would generate. Basically, most of its surface consisted of these connectors, and all transmission lines were placed on these layers as well. This meant that, instead of the usual striplines, microstrip lines were used. Because of that, there was a huge change in characteristics between the board designed for this project and this test board. Still, some valuable insights were believed to be gained from this experiment. A 3D model of the board is shown in Appendix B.

SIMULATIONS AND MEASUREMENTS

There were already excellent simulation models in *Ericsson's* database for this board, so nothing had to be constructed from scratch. It was possible to just select some conductors and simulate the S-parameters directly. But still, this was when the first problem was encountered; for even though special dielectric materials can be requested when ordering a PCB, the manufactures do not guarantee that these will be used. The result is that the dielectric constant may differ from what was expected. This in turn meant that (according to (6.7) and (6.8)) the frequency spectrum will be changed. Since the simulated values were to form the basis for

the signal processing, an unknown dielectric constant was very troublesome.

The simulations were carried out with ϵ_r equal to 4.3 (the number selected by the designers). Two closely located conductors were chosen, and the 4 S-parameters for them were analyzed. The simulated crosstalk is shown in figure 8.5 below.

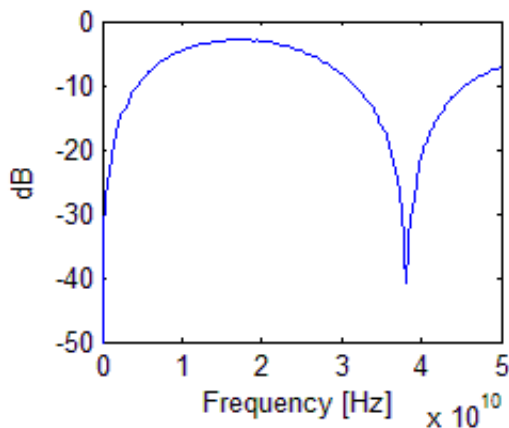


Figure 8.5. The S-parameter for the simulated crosstalk.

As can be seen in the figure, the crosstalk is much stronger for this transmission line, than for the *measurement structures* implemented in the previous chapter. This is mostly due to the fact that it relates to a microstrip (a trace on a PCB's surface) and not a stripline (a buried trace). In order to test the simulation, the circuit crosstalk was also measured with a network analyzer and the result can be seen in figure 8.6. Also included is the simulation for ϵ_r equal to 3.7, since this value gave a simulation that was more in line with the measured data.

The test was to be carried out for a data rate of 10 Gbit/s, meaning that most of the signal content would reside below 10 GHz. For that reason, it was not as vital to get good comparisons between the simulated and the measured data for higher frequencies.

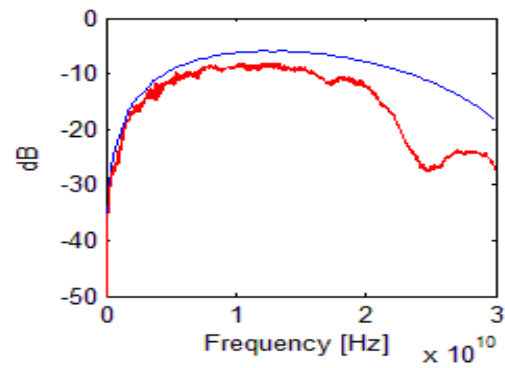


Figure 8.6. A comparison between the simulated (blue) and measured (red) crosstalk.

RECONSTRUCTING THE SIGNAL

The test setup is described in figure 8.7 below.

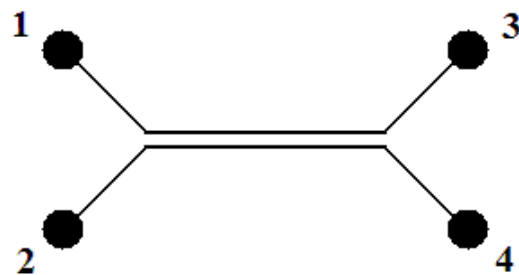


Figure 8.7. The test setup; four different inputs/outputs, and two conductors with middle sections close enough to generate crosstalk.

Connector 1 was attached to a signal generator, connectors 3 and 4 were connected to an oscilloscope and connector 2 was terminated by a 50 Ω resistance.

The signal generator was programmed to produce a pseudo random binary sequence at 10 Gbit/s, and the amplitude was set to about 275 mV. Using the previously described approach with Fourier series analyzes, the measurements captured in connector 4 was analyzed and operated upon. The input signal (or more accurately; the output signal from connector 3) is shown in Figure 8.8. In Figure 8.9 the measured output from connector 4 is shown, and the processed signal is shown in figure 8.10.

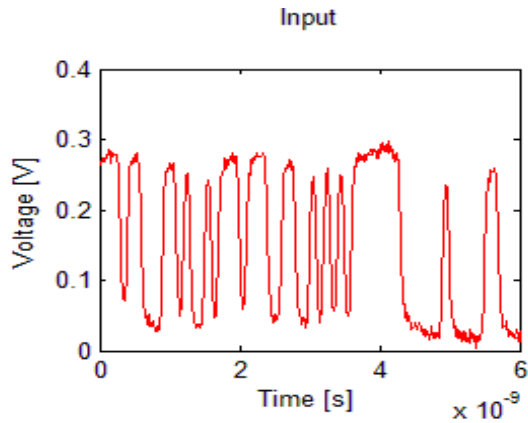


Figure 8.8. The output from connector 3.

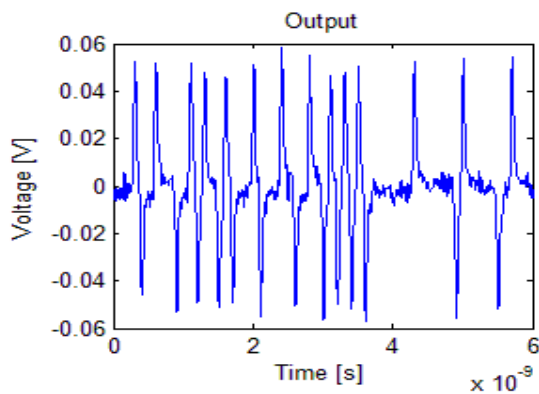


Figure 8.9. The output from connector 4.

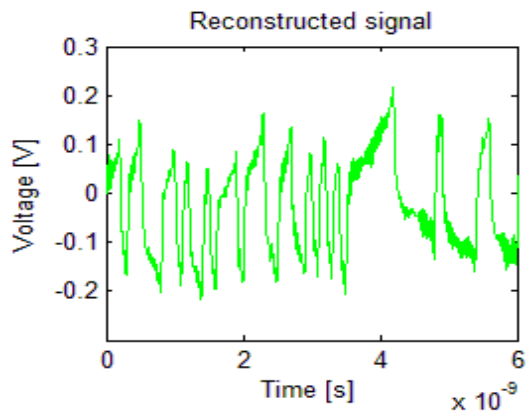


Figure 8.10. The reconstructed signal.

As can be seen, there are severe differences between the reconstructed and the original signal. This was at the time believed to be due to many reasons, most notably errors in the simulation and the effect of the SMP connector (it was not de-embedded).

But still there were several details that the software seemed to reconstruct nicely; all the

flanks of the signal are captured really well, and they are also placed on the appropriate position along the time axis. If the segments where the signal's derivative is close to zero could be evened out, than it would look quite similar to the input signal. But since the fault seems to be integrated along the time axis, it eventually looks quite different from the original signal.

FAULT SEARCHING

In order to evaluate why there was a difference between the actual and the desired results, two things were done. First of all the transfer function, $H(f)$, from connector 3 to connector 4 was derived with MATLAB. This was done in frequency domain, using the relationship in (8.4). $U_3(f)$ and $U_4(f)$ are the measured signals at the respective connectors.

$$U_3(f) \cdot H(f) = U_4(f) \rightarrow \frac{U_3(f)}{U_4(f)} = H(f) \quad (8.4)$$

Once again it must be stressed that $U_3(f)$ is not the actual input, and also that the derived transfer function incorporates noise. Hence, $H(f)$ was not the perfect transfer function, but it would still contain some useful information. The transfer function between 0 and 10 GHz can be seen in figure 8.11 below.

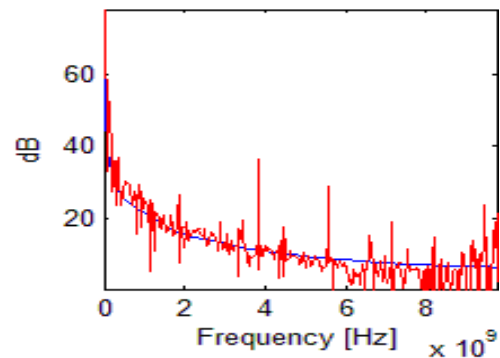


Figure 8.11. $H(f)$ (red) from 0 to 10 GHz, the simulated curve (blue) is also depicted.

The function may look chaotic, but it is actually not very far from the simulated values (apart from some of the sudden peaks). But if instead the phase is shown, the difference becomes more apparent. This is depicted in figure 8.12.

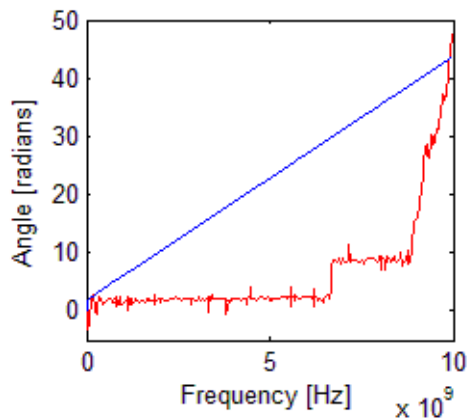


Figure 8.12. The phase for $H(f)$ (red) and for the simulated function (blue) from 0 to 10 GHz.

As could be seen; the difference in phase is huge and a possible explanation for the unsatisfactory results. Because of this, attempts were made to change the phase and thereby improving the reconstruction software. Several changes were made, but one in particular stood out: If $S_{inv}(f)$ was replaced with its complex conjugate (i.e. multiplying the phase with -1), then the results in figure 8.13 were obtained.

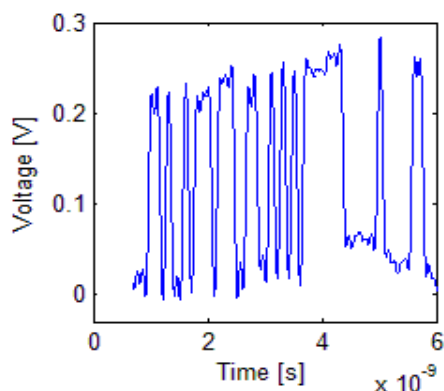


Figure 8.13. The reconstructed signal, when the simulated $S_{inv}(f)^*$ was used, to simplify comparison; an offset has been added to the signal.

It would turn out that using the complex conjugate of the analytically correct transfer function was the best solution. And, since the better results were general, the method was used from this point on. No explanation was found as to why the improvement occurred.

FREQUENCY CONTENT VERSUS RECONSTRUCTION QUALITY

In the *Theory* chapter it was described that the signal reconstruction with *Fourier series analyzes* may approach perfection as the length of the used frequency spectrum approaches infinity. In reality this usually means that a perfect reconstruction is impossible, and this is the case for this thesis project. However, an attempt to find out an appropriate length of the used spectrum could easily be made by making a generated signal pass through a digital low pass filter. The following figures show the results for a 10 Gbit/s signal. First, in figure 8.14, an unmodified 10 Gbit/s signal is shown (the reason for its somewhat distorted looks is that it has been propagated through two *vias*). Figures 8.15-8.17 show the signal compared to filtered ones.

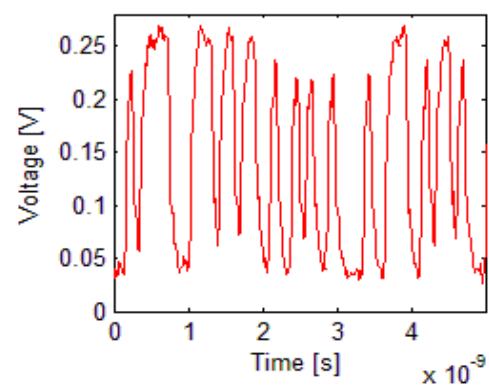


Figure 8.14. The unmodified 10 Gbit/s signal.

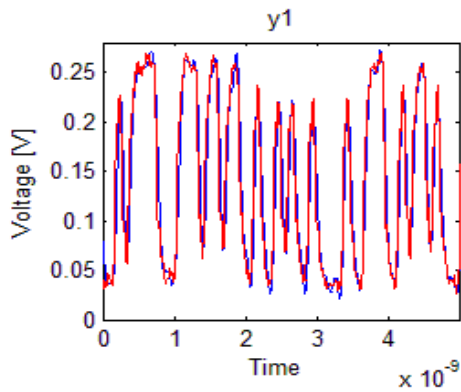


Figure 8.15. The unfiltered signal (red), and the signal filtered through an 8 GHz low pass filter.

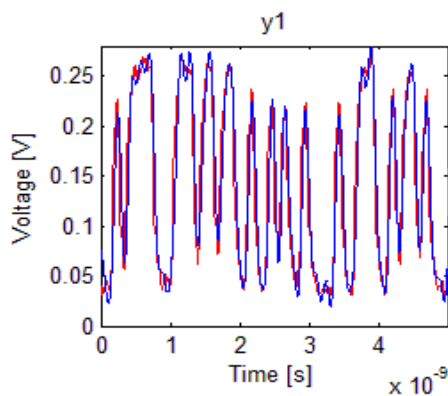


Figure 8.16. The unfiltered signal (red), and the signal filtered through a 7 GHz low pass filter.

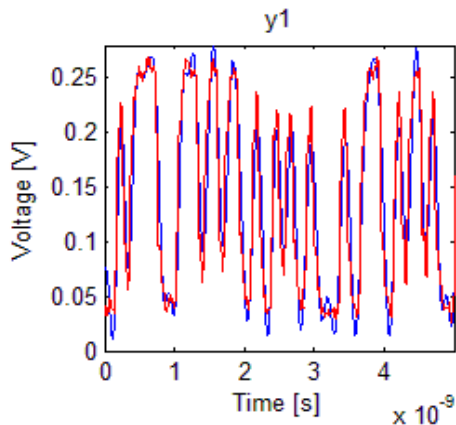


Figure 8.17. The unfiltered signal (red), and the signal filtered through a 6 GHz low pass filter.

It is apparent that the difference between the original signal and a signal passed through an 8 GHz low pass filter is very small. At 7 GHz there are some small differences, and at 6 GHz the difference becomes problematic. These

results mean that it was essential for the transfer function to be correct up to about 7 GHz for a 10 GBit/s system, and the remaining spectrum will be less important. This would prove to be a vital guideline in the remaining parts of the project.

As a final note regarding the 26Gbit/s system; the reason why similar measurements have been excluded will become apparent later on in the report.

9. MEASUREMENTS

This chapter will be devoted to describing the measured results from implemented test structures. Once the board had been manufactured the connectors were soldered onto the surfaces, and a network analyzer was used to retrieve the S-parameters.

Later on, signals from both the *applied test points* and *experimental test points* were collected and connected to the signal processing software. The results were evaluated, and some examples of the reconstructed signals will be shown in this chapter.

S-PARAMETERS

T-SHAPED STRUCTURES- 10 GBIT/S

These structures did somewhat yield the expected results, especially for lower frequencies. Measured S-parameters, for the 10 Gbit/s structure with the *victim line* and the *target line* placed on adjacent layers is shown in figure 9.1 along with the simulated ones. The difference between this simulation and earlier ones is that all *vias* and cables are now included.

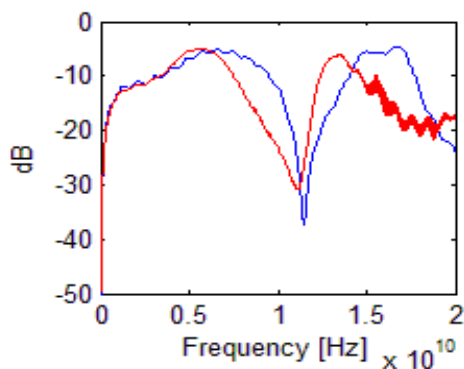


Figure 9.1. A comparison of the S-parameters for the simulated measurement structure (blue) and the actual circuit (red). The measurement structure is broadside coupled.

A similar comparison is shown in figure 9.2 below, but it shows the circuit with the edge coupled *measurement structure*.

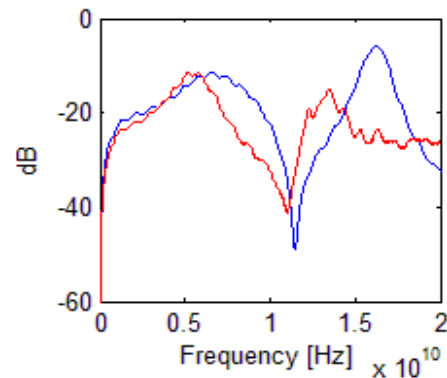


Figure 9.2. A comparison of the S-parameters for the simulated measurement structure (blue) and the actual circuit (red). All circuitry is placed on the same layer.

It is clear that the simulations were right on one thing; placing the measurement structure above or below the *victim line* will not change the general behavior of the curve, but only increase the strength of the crosstalk.

T-SHAPED STRUCTURES- 26 GBIT/S

The results for the T-shaped structure, designed for 26 Gbit/s were not as satisfactory. The simulations had not captured the correct behavior for the frequency spectrum needed to reconstruct the signal. According to my supervisor this was not an unexpected fact; the *vias* were expected to heavily affect the signal for higher frequencies, and likely in an unpredictable fashion.

The resulting S-parameters for the two structures are shown in figure 9.3 and figure 9.4, along with made simulations. Once again the simulations were accurate about the fact that a general difference in magnitude would be the main difference between them.

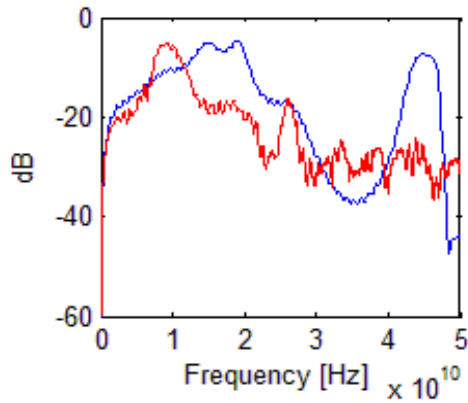


Figure 9.3. A comparison between the simulations (blue) and the measurements (red) for the T-shaped 26 Gbit/s structure. The measurement structure is placed on an adjacent layer.

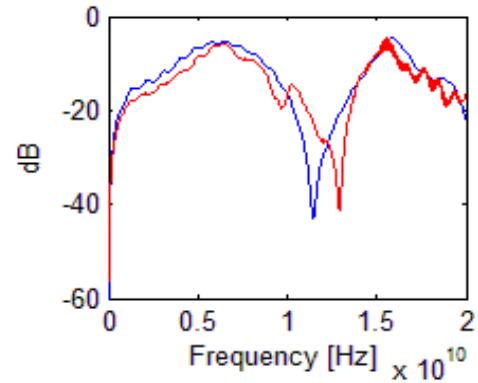


Figure 9.5. One of the measured transfer functions (red) for the L-shaped measurement structure, and the simulation (blue).

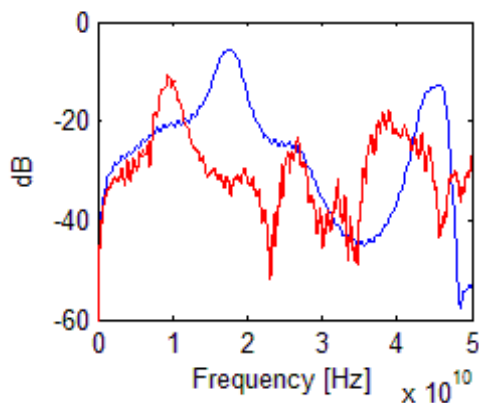


Figure 9.4. A comparison between the simulations (blue) and the measurements (red) for the T-shaped 26 Gbit/s structure. The victim and target lines are placed on the same layer.

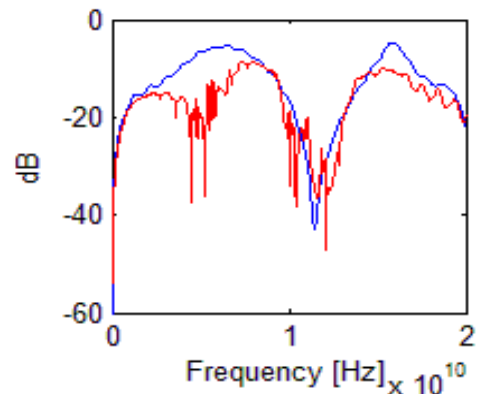


Figure 9.6. Another one of the measured transfer functions (red) for the L-shaped measurement structure, and the simulation (blue). The reader should notice the difference between them.

L-SHAPED STRUCTURES

This structure proved to be the most difficult to evaluate, and this was because of the unpredictability the structure gave. Some measured S-parameters would yield a fairly good accordance with the simulations, while others would not. In the following figures (9.5-9.6) two very different outputs are shown. These transfer functions should, according to the theory, be identical.

Unfortunately, one of the *experimental test points* (the edge coupled, L-shaped structure) was destroyed during the soldering process, and could not be used to retrieve the S-parameters. Still, the remaining structure made four different transfer functions available and the assumption was made that the difference between the two L-shaped structure would only be a constant difference in magnitude.

The conclusion was that the L-shape, though it according to simulations would hold some value, was not reliable enough to earn a real recommendation for wider use. But it should

be stated that the available data was not enough to conclusively dismiss the shape.

THE PROPAGATION PATH

As, briefly, described in the *Implementation* chapter; a structure for testing the importance of the propagation path was included in the PCB. Basically the setup was as following: One path was more or less straight, while the other was curved in a way that could result in crosstalk with itself. This experiment was important to determine in what way the propagation path between the *measurement structure* and the *via* would influence the performance.

A central theme within this thesis is that the risk for crosstalk and other disturbing effects increases with the frequency, and this seemed very true for this experiment as well. In figure 9.7 the measurements from the experiment are shown; the propagation path does not seem to have any significant effect upon the signal until around 30 GHz (the difference below that is probably mostly due to the soldering or other manufacturing faults).

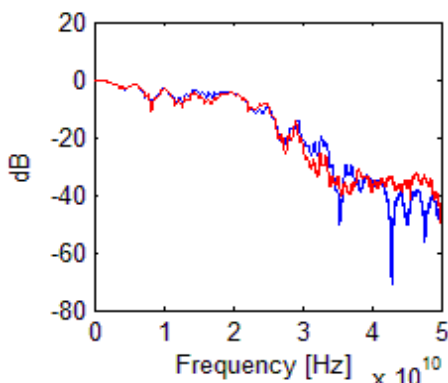


Figure 9.7. The S-parameters for two different propagation paths of equal length; one curved (blue) and one somewhat straight (red).

RECTANGLE SHAPED STRUCTURES

Once again a structure was damaged during the soldering process, and this time it was the

rectangle shaped structure designed for 26 Gbit/s. A reasonable assumption regarding these not obtained measurements is that the relation between the two rectangle shaped structures would have been the same as the relation between the broadside coupled, T-shaped 10 Gbit/s and the 26 Gbit/s structures.

As for the performed measurement; it turned out that this structure yielded surprisingly stable results, and for lower frequencies, quite good accordance with the simulation [stable, in this case meaning general]. Figure 9.8 shows the measured results, in comparison to the simulated ones.

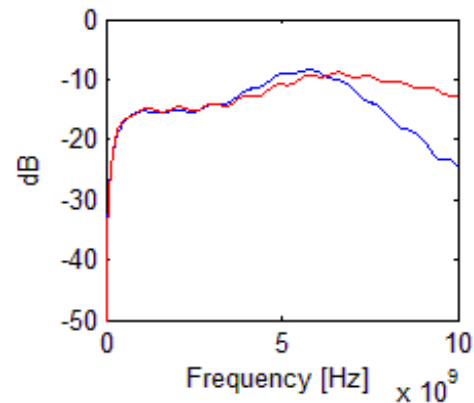


Figure 9.8. The measured S-parameters (blue) and the simulated (red) for a rectangle structure (10Gbit/s).

Since the rectangle shaped measurement structure gave such stable results, they seemed to be good candidates for future use.

USING THE RECONSTRUCTION SOFTWARE

Using the program *Non Contact Test Point ANALYZER* (the produced software, that will be described in the next chapter), some different measurements were analyzed.

THE 26 GBIT/S PROBLEM

As could be seen earlier, the S-parameters for the 26 Gbit/s structures were far from

expected, and unfortunately it proved impossible to fully use the 26 Gbit/s adapted *measurement structures*. The main reason for all of this was that the *vias* the signal passed through acted like stubs. Since stubs have a larger effect upon signals with higher frequency content, the 26 Gbit/s signals were much more influenced than those with 10 Gbit/s. In order to avoid this problem in the future, recommendations were made to always use *buried vias* when implementing this structure. But since no use could be made of the 26 Gbit/s *measurement structures*, they are from this point on excluded from the chapter.

EXPERIMENTAL TEST POINTS

Since the transfer functions for these measurement structures had already been obtained, they could be used to recreate the signals that were inserted into the *source lines*. In the following example a 10 Gbit/s signal is measured by the broadside coupled T-shape, and the reconstructed signal may be seen in figure 9.9. In figure 9.10, an eye pattern of the reconstructed signal has been generated by the software.

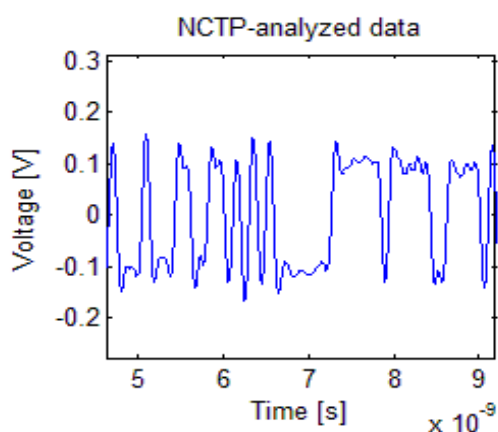


Figure 9.9. The reconstructed 10 Gbit/s signal.

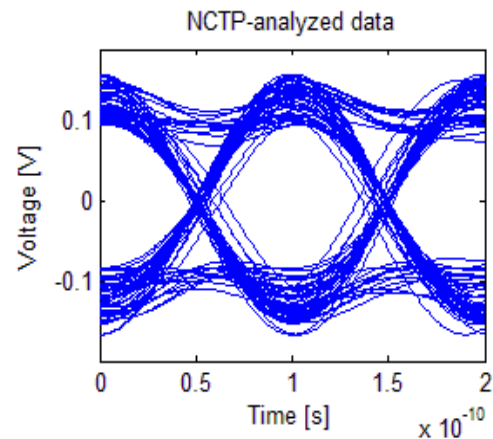


Figure 9.10. The reconstructed 10 Gbit/s signal's eye pattern.

Regrettably, there are no input values to directly compare the generated pattern with. But since the PRBS (that constituted the input) came directly from a signal generator, some knowledge was available. The amplitude is captured very well by the reconstruction, and the eye diagram looks very accurate as well. There is little doubt that the constructed signal mimics the real one quite well, but since the correct transfer function was available that is hardly surprising.

Also the rectangle shaped measurement structure was able to capture enough information to allow an accurate reconstruction. In order to create a common mode signal, the following trick was used: the two *source lines* were fed with a differential signal, but there was a small time difference between these lines. For instance; if the signal shifts from high to low, then the small time difference between the lines will create short spikes for the measurement structure. An example of this is shown in figure 9.11 below.

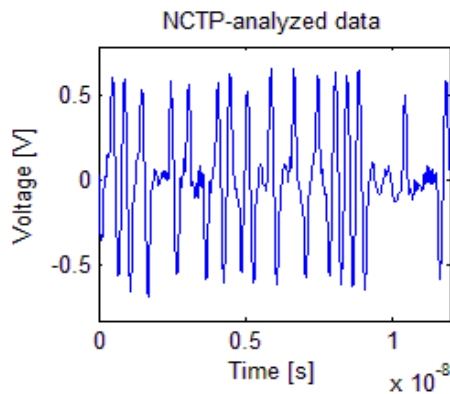


Figure 9.11. The reconstructed common mode signal.

The sharp peaks are just what would be expected from a reconstructed signal, and, though the parts where the voltage should be constantly zero (e.g. around 1 ns in the figure) seem to oscillate a bit, there is little doubt that the measurement structure works.

APPLIED TEST POINTS

One thing that has not yet been mentioned is that the *applied test points* were applied to *source lines* suspected of carrying an undesired common mode signal. This gave the opportunity to test the rectangle shaped structure in reality. Obviously, the T shaped structures could be used for common mode measurements as well. The results were promising, but not perfect. In figure 9.12 a common mode signal is measured and in figure 9.13 the resulting spectrum of an fft analysis (of the reconstructed signal) is shown.

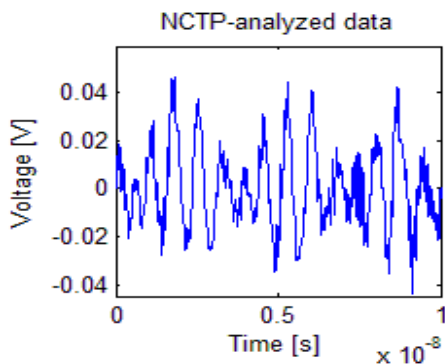


Figure 9.12. The reconstructed common mode signal.

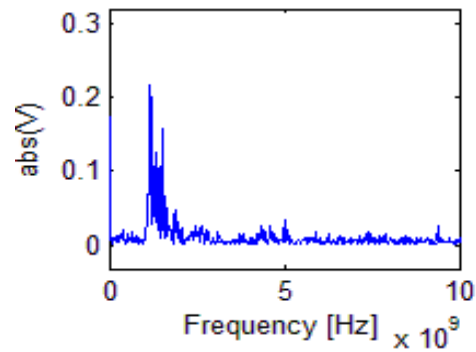


Figure 9.13. An FFT analysis of the reconstructed common mode signal.

There is clearly something being measured, and according to the frequency analysis, its main component resides around 1.1 GHz. Unfortunately, the signal was believed (with good reasons, that will not be explained in this thesis) by *Ericsson* to have a main frequency component of 937.5 MHz. Still, something has clearly been measured and more work will have to be done in order to explain the difference in frequency.

As for the attempts to measure differential signals, they were also quite successful. The reader will have to keep in mind that 10 Gbit/s *measurement structures* were applied to 2.5 Gbit/s signal traces, and that not optimized transfer functions were used. Still, as shown by the example in figure 9.14 below, the results were fairly satisfactory.

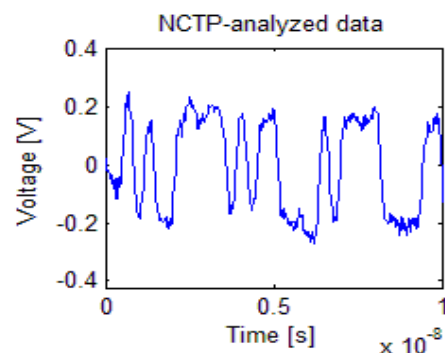


Figure 9.14. A reconstructed 2.5 Gbit/s signals from the applied test points.

It is impossible to know for certain how accurate this reconstruction actually is, but

the shape looks very probable. But, as the reader may notice, the entire signal is a little bent, which probably is a result from inaccuracy of the transfer function for some lower frequencies. This came to generate huge problems when studying the eye pattern, as can be seen in figure 9.15.

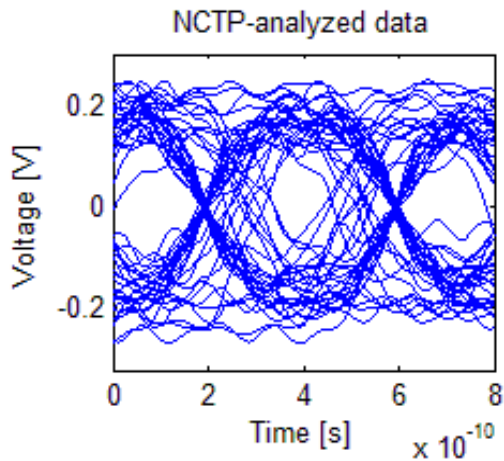


Figure 9.15. *The reconstructed 2.5 Gbit/s signal's eye pattern.*

The created software assumed the signal to constantly oscillate around 0 V, showing the importance of having accurate S-parameter data.

But all in all, the verification measurements, in many ways, went far better than expected and, though some work will remain after this project is concluded, they showed the potential of the measurement system.

10. THE FINAL PROGRAM

Along with the report and the software, a user's guide for the signal processing program was handed to Ericsson. If the reader wishes to study the program in more detail, a copy has been included in Appendix C.

NON CONTACT TEST POINT ANALYZER

The program, delivered to *Ericsson*, was named *Non Contact Test Point ANALYZER* and designed to be the first iteration in a line of programs. Hence, the code was deliberately written so that additional functions could be implemented after this thesis project's completion.

DESCRIPTION

Implemented by the MATLAB GUI editor, the program consisted of simple push buttons, radio buttons and two graphs (one displaying raw data and another one showing the reconstructed signal). Three different types of measurements were implemented; *Entire segment*, *Eye*, and *Binary info measurement*. The *Entire segment* option was the basic reconstruction of the original signal, *Eye* would first recreate the signal and then generate an Eye measurement while the third option, *Binary info measurement*, would recreate the signal and remake it into strict 1's and 0's.

The user is asked to load S-parameter data and the program requires the data to be in the form of a .s*p file (a special file type, used to store S parameter data), but no requirement is set on the number of frequencies it must contain (though equal spacing between them is assumed). It is also possible for the user to decide what frequency spectrum will be used.

After the user has loaded the measured data, the program begins the reconstruction

process. If everything has worked properly, one graph will now show the measured data while the other shows the reconstructed signal.

For a more extensive description of the features included in the program, the reader is once again referred to Appendix C.

PERFORMANCE

As concluded earlier, the quality of the results depended on how well the simulated S-parameters imitated the real ones and it is therefore difficult to evaluate this program's performance from that aspect. It is better to test how time consuming the analysis was and how well it handled larger sets of data. For both these criteria the results were quite satisfying. The program automatically divided the data into smaller pieces of preset sizes, and this meant that the computational time would grow more or less linear with the data size.

ACKNOWLEDGMENTS

Obviously MathWorks (developer of MATLAB) has been the largest contributor to this code, and extensive use of the included toolboxes was made (especially *Signal processing*). But apart from the major corporations, the biggest contribution came from a small program called *read_in_s_param.m* that was designed by my supervisor Ingvar Karlsson. The program's purpose was to import the S-parameters stored in *Touchstone* files into the MATLAB environment. Being given this program simplified my task immensely.

CONCLUSIONS

This program was not a very complex structure; the number of rows that the code contained was surprisingly few. Still, the program did what it was designed for and the

code was structured so that it could easily be expanded or changed. Also, the interface was very user friendly and, combined with a help menu, the program could be considered to have fulfilled *Ericsson's* criteria of "simple usage".

All of this combined with its performances regarding speed and stability makes it fair to conclude that this part of the project was a success.

11. CONCLUSIONS

THE PROJECT

To summarize the conclusions made during this project is not an easy task. Some geometric recommendations have been handed to *Ericsson* in a separate report, along with other manufacturing and production advices.

However, some of the more important discoveries should be mentioned, such as the technology's promising results (for the T and rectangle shaped structures), the success of the created signal processing software and the low load disturbance placed upon the *source lines*.

Still some questions were never answered, the biggest one being why the complex conjugate of the calculated transfer function gave so much better results than the analytically correct one, and also why the L-shaped structure failed in such a surprising way.

If I would have to conclude whether the project was a success or a failure, I would call it a success. It has been proven that the *measurement structures* implemented received enough information to make a good reconstruction of the signal, it has been proven that the structures were capable of measuring bit rates that they were not designed for and it has also been proven that the calculations needed to perform the reconstruction can be made to increase in a linear relation against the measured data which in turn will promise the possibility of real time analysis.

One thing that has yet not been mentioned is that the test *vias*, which were implemented on the board, were never used. This was because of time constraints and the surprisingly good results that could be reached without de-

embedding them. Still, since the board remains intact, they could prove a future asset.

To summarize the entire project might not have been an easy task, but summarizing this small section of this short chapter is; non contact test points show great potential in becoming a valuable part of future PCB design.

FUTURE WORK

The work with *non contact test point* has had a good start, but much work remains before it can be considered completed. Using the measured S-parameter with the software showed that the system has great potential, and that the *measurement points*, implemented in the hardware, receive enough crosstalk to make a fairly accurate reconstruction.

Though nothing has been decided yet, I hope to continue work on this project and refine the system. So far every encountered problem has been dealt with in an arbitrary fashion, but the procedures need to be streamlined. This will include setting up predefined structures for the layout teams to follow, along with more accurate simulations. Everything can be included in a single digital folder, so that it can be quickly accessed by any *Ericsson* employee.

Hopefully I will be able to implement the 26 Gbit/s *measurement points* on a board where *buried vias* are available. This would drastically improve the performance, and the accuracy of the simulation. Such, more expensive features, will probably be a necessity for the higher bit rates. "Luckily", it is not only this small measurement structure that suffers from the effect of *stubs*, and it is a safe assumption that the industry will be, more or less, forced to allow costly solutions. This,

combined with the increasingly problematic probe based measurements, promises a positive future for these types of solutions.

I also believe it is possible that certain other parts of this project would have been simpler to do in a couple of years; a lot of experienced engineers have expressed their inexperience with how circuits behave at higher frequencies, it seems that the industry may have a lot to learn. This will likely lead to more accurate software, and thereby more accurate simulations, which in turn will yield better predictions. As of now, I and other users often encountered bugs in different simulation software, making the results less reliable. Hopefully, these encounters will be fewer in future software editions.

REFERENCES

- [1] D. J. Griffiths, *Introduction to electrodynamics*, third edition, San Francisco, USA, Pearson Benjamin Cummings, 2008
- [2] P. H. Young, *Electrical communication techniques*, fifth edition, Upper Saddle River, USA, Pearson Prentice Hall, 2004
- [3] D. Sjöberg and M. Gustavsson, *Kretsteori, ellära och elektronik*, second edition, Lund, Sweden, Lunds Tekniska Högskola, 2008
- [4] A. Karlsson and G. Kristensson, *Microwave Theory*, Lund, Sweden, Lunds tekniska högskola, 2009
- [5] T. Glad and L. Ljung, *Reglerteori*, second edition, Studentlitteratur, Lund, Sweden, 2003
- [6] B. Gustavsen and A. Semlyen, *Rational Approximation of frequency domain responses by vector fitting*, IEEE Transactions on power delivery, Vol. 14, 1999
- [7] H. W. Johnson and M. Graham, *High-Speed Digital Design*, Englewood Cliffs, PTR Prentice-Hall Inc. 1993
- [8] S. H. Hall, G. W. Hall and J. A. McCall, *High-Speed Digital System Design*, New York, USA, John Wiley & Sons Inc., 2000
- [9] T. Williams, *EMC for product Designers*, second edition, Oxford, The United Kingdom, Newnes, 1996
- [10] C.R. Paul, *Electromagnetic Compatibility*, New York, USA, John Wiley & Sons Inc., 1992
- [11] T. Zelder, H. Rade, and H. Eul, *Contactless electromagnetic measuring system using conventional algorithms to determine scattering parameters*, Institut für Hochfrequenztechnik und Funksysteme, Universität Hannover, Germany, 2007
- [12] K. Yhland, J. Stenarson and C. Wingqvist, *Non contacting measurement of reflection coefficient and power in planar circuits up to 40 GHz*, SP Technical Research Institute of Sweden, 2007
- [13] Agilent Technologies Inc, *De-embedding and Embedding S-parameter Networks Using a Vector Network Analyzer*, USA, 2004
- [14] S. Lucyszyn, C. Stewart, I.D. Robertsson and A.H. Aghvami, *Measurement techniques for monolithic microwave integrated circuits*, Electronics and Communication Engineering Journal, April 1994
- [15] Agilent Technologies Inc, *Agilent technologies Infiniium 90000 X-Series Oscilloscopes Data Sheet*, USA, 2011
- [16] Tektronix Inc., *Effects of Measurement Fixtures On S-parameter Compliance Testing of Infiniband Cable Assemblies*, USA, 2005
- [17] G.E. Bridges, *Non-Contact Probing of Integrated Circuits and Packages*, Microwave Symposium Digest, Vol. 3, 2004
- [18] C.J. Falkingham, I.H Edwards and G.E. Bridges, *Non-Contact Internal-MMIC Measurement using scanning force*

- probing*, Microwave Symposium Digest, Vol. 3, 2000
- [19] K. Yhland, J. Stenarson and C. Wingqvist, *In-circuit, Non-Contacting, S-parameter measurement for planar circuits*, Chalmers University of Technology and SP Swedish National Testing and Research Institute, 2001
- [20] Sugawara K, C.P. Chen, Z. Ma, T. Anada and D.W.P. Thomas, *Non-contacting Electric and Magnetic Field Probe for Measuring EM Fields on Microwave Planar Circuits*, Microwave Conference, 2007. APMC 2007. Asia-Pacific
- [21] S.S. Osofsky and S.E. Schwarz, *Design and Performance of a Non-Contacting Probe for Measurement and High-Frequency Planar Circuits*, IEEE transactions on Microwave Theory and Techniques, Vol. 40, issue 8, August 1992
- [22] H. You and M. Soma, *Crosstalk Analysis of Interconnection Lines and Packages in High-Speed Integrated Circuits*, IEEE Transactions on Circuits and Systems, Vol. 37, No. 8, August 1990
- [23] A. Deutsch, H.H. Smith, C.W. Surovic, G.V. Kopcsay, D.A. Webber, P.W. Coteus, G.A. Katopis, W.D. Becker, A.H. Dansky, G.A. Sai-Halasz and P.J. Restle, *Frequency-Dependent Crosstalk Simulation for On-Chip Interconnections*, IEEE Transactions on Advanced Packaging, Vol. 22, No. 3, August 1999
- [24] J.R. Yeargan, R.L. Day and T. Nguyen, *Crosstalk in Multilayer Printed Circuit Boards*, IEEE Transactions on Education, Vol. 31, No. 2, May 1988
- [25] A.A Ruehli and H. Heeb, *Circuit Models for Three-Dimensional Geometries Including Dielectrics*, IEEE Transactions on Microwave Theory and Techniques, Vol. 40, No. 7, 1992
- [26] T. Sakurai and K. Tamaru, *Simple Formulas for Two- and Three-Dimensional Capacitances*, IEEE Transactions on Electrical Devices, Vol. ED-30, No. 2, February 1983
- [27] J.H. Chern, J.H. Huang, L. Arledge, P.C. Li and P. Yang, *Multilevel Metal Capacitance Models For CAD Design Synthesis Systems*, IEEE Electron Device Letters, Vol. 13, No. 1, January 1992
- [28] K. Yhland and J. Stenarson, *Non contacting Measurement of Power in Microstrip Circuits*, 67th ARFTG conference June 2006
- [29] M.I. Montrose, *EMC & the Printed Circuit Board: Design, Theory & Layout made simple*, first edition, New York, Institute of Electrical and Electronics engineering Inc., 1999
- [30] *Allegro® Design Entry Foundations BPC training for Ericsson book 1*, Cadence Design Systems Inc., USA 2008
- [31] P. Carlson and S. Johansson, *Elektronisk mätteknik – Generella mätinstrument*, second edition, Liber AB, Stockholm, Sweden, 1989
- [32] R. Bansal, *Handbook of Engineering Electromagnetics*, First edition, Marcel Dekker Inc., New York, USA, 2004
- [33] R.L. Fante, *Signal Analysis and estimation- An introduction*, First edition, John Wiley & Sons Inc., Wilmington, 1988

[34] K. Mitzner, *Complete PCB Design Using OrCAD® Capture and Layout*, First edition, Elsevier Inc., Oxford, The United Kingdom, 2007

[35] Agilent Technologies Inc, *Agilent 71501D Eye-Diagram Analysis User's Guide*, Santa Rosa, USA, 2002

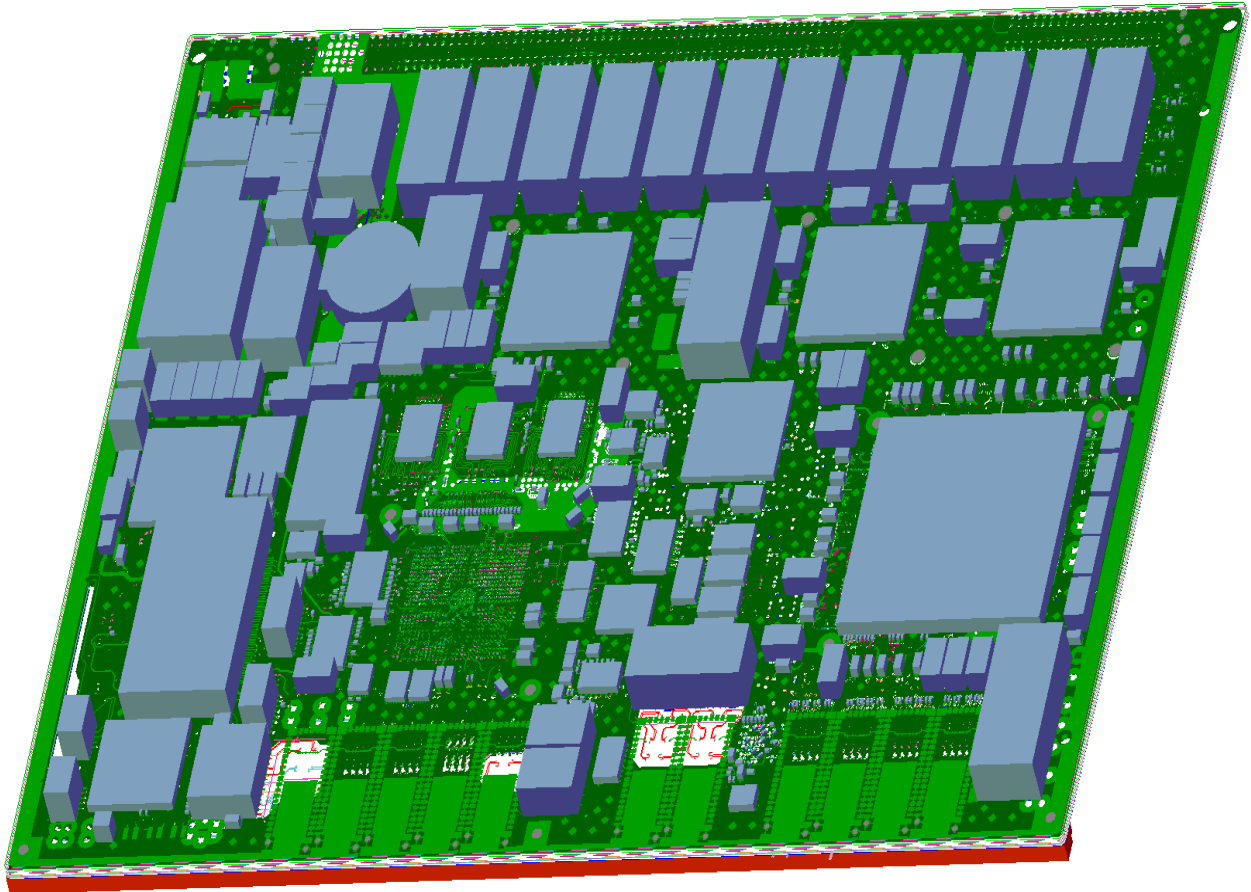


Figure A.1. A 3D generated view of the SCXB board.

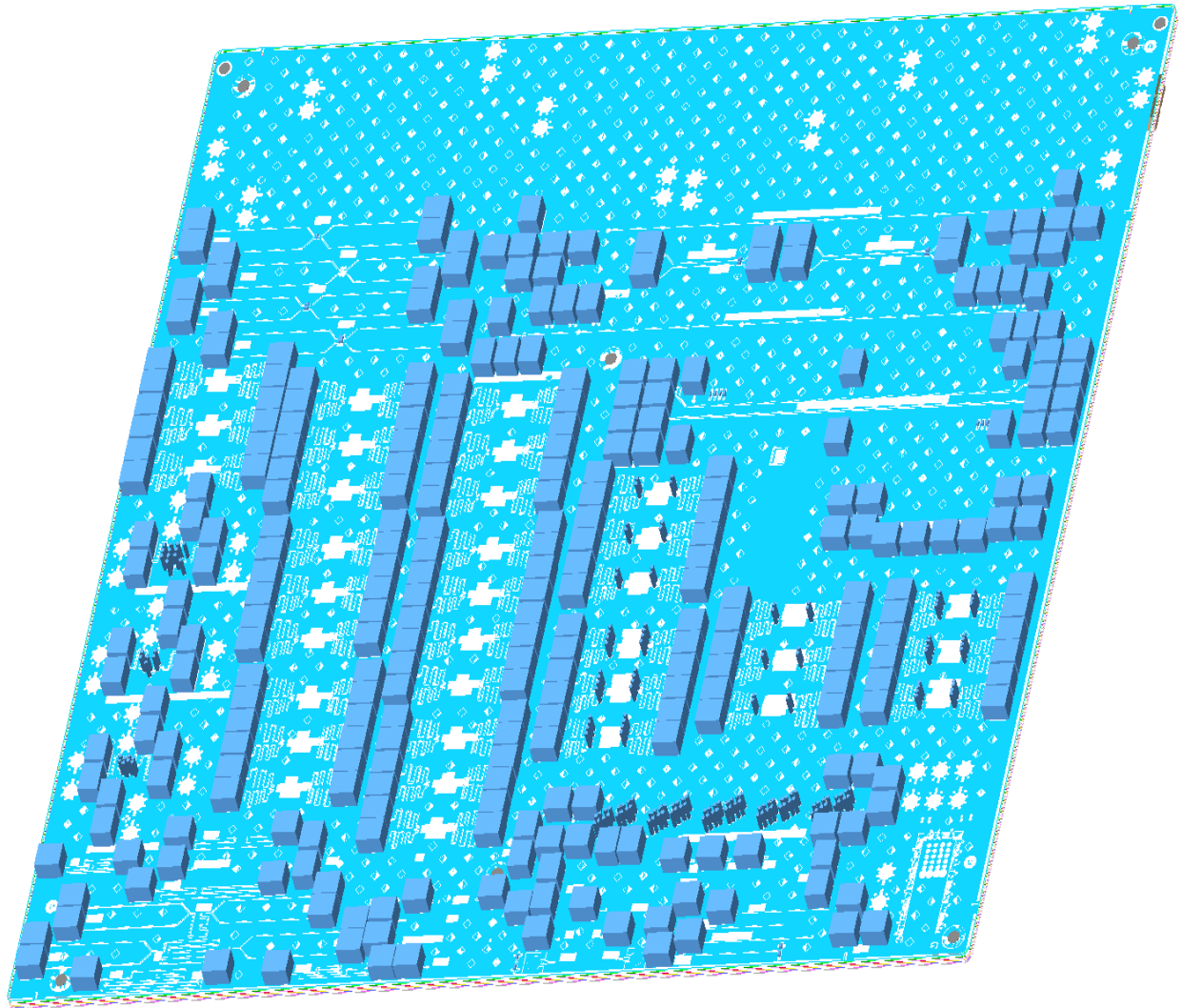


Figure B.1. A 3D generated view of the SMP connector test board. The blue boxes are the auto generated symbols of the connector, the reader should notice how plentiful they are on this board.

Non Contact Test Point ANALYZER

-----USER'S GUIDE-----

Version 1.0

INTRODUCTION AND PREPARATIONS

The program is a GUI created with the MATLAB GUI editor, it is designed to be easy to use and reliable in performance. Its purpose is to enable contact free measurements of internal signals within a PCB, by supplying the software capable of recreating the original signal if given enough information.

Most of the software was designed here at Ericsson, but much use was made of the *Signal processing toolbox*, supplied by MathWorks. One requirement to run this program is that the *MATLAB Compiler Runtime* (MCR) is installed upon the system. If problems are encountered during the installation process, please visit <http://www.mathworks.se/help/toolbox/compiler/f12-999353.html#bs5vv3i> for additional support. Also, the auto generated *readme.txt* file, which is created when a MATLAB standalone program is compiled, contains some information of the installation process (the file is included in the folder). Apart from that, everything that is required to use this program may be found in the supplied folder, and that folder may be placed anywhere on the hard drive.

REQUIREMENTS

This particular standalone program is designed to function in a Windows based environment, be it a PC or an oscilloscope. When it comes to hardware requirements, no lower boundary is defined; since the program does not contain any heavy graphic and the MATLAB functions are somewhat optimized, the program should run smoothly on most processors encountered in the industry today. It is in this guide assumed that the user is equipped with a mouse (required) and a keyboard (optional, but strongly recommended).

Using the program will require two different input files; a *.s*p* file and a text document containing at least two columns of data (time and measured voltage, in that order). It is also possible to have the program analyzing a text document with three columns, when e.g. a differential pair is measured. But this will be described in detail later on. This means that a well structured text file for a single ended measurement may start (or finish) like this:

```
-5.01767E-09 7.8586E-02  
-5.01689E-09 7.8544E-02  
-5.01611E-09 7.8502E-02
```

-5.01532E-09 7.8418E-02

-5.01454E-09 7.8354E-02

Exactly what the data file looks like after it has been exported from the oscilloscope may vary between different manufacturers. But the user is advised to always strive after the “cleanest possible alternative, and always avoid saving it in files that cannot be opened by standard text programs (e.g. Notepad and Wordpad).

To what extent the recreated shape will mimic the original’s depends on how accurate the transfer function in the .s*p is. The user may by him/herself decide how to obtain this file, as long as it is of standard Touchstone format, it makes no difference whether it originates from a simulation or a measurement.

It is also advantageous to have a lot of frequency points in the file, as the linear interpolation between them (performed by the software) may be less accurate than an expanded simulation. However, though there is a significant difference between a transfer function containing 500 points and one containing 5000, increasing it above a certain number does not buy you that much. I.e. do not expect the same improvement between 50,000 and 100,000 points. Still, an appropriate limit is impossible to give for the general case, so unfortunately it will be up to the user to determine it for each individual case.

Since the lower parts of the frequency spectrum will play a vital role in the software’s execution, it is important the lowest frequencies, covered within the file, are positioned close to 0 Hz. Though it according to the mathematical theory would cause problems to have a point placed precisely at 0 Hz, the software has been designed to cope with it.

It is important to note that the software assumes the points to be linearly placed along the frequency axis, so do not use any “adaptive” features when starting the simulation. Since the program only checks the position of two frequency points (which is enough to predict the rest, if there is an equal distance between all neighboring points) an “adaptive” placement would lead to great errors when operating in the frequency domain.

A similar assumption is made about the text file, containing the data; only the first two rows in the time column is used, the rest is auto calculated. This, of course, also means that in the case when there are two voltage columns; both samples on each row must relate to the same time. The program does not support multiple time columns. But no restrictions are made about exceeding the number of columns, as long as the ones that are used contain the necessary information.

When it comes to the length of the text file (and thereby the length of the data), no upper limit exists. The program’s execution time is almost directly proportional to the data size, meaning that twice the signal length equals twice the computation time.

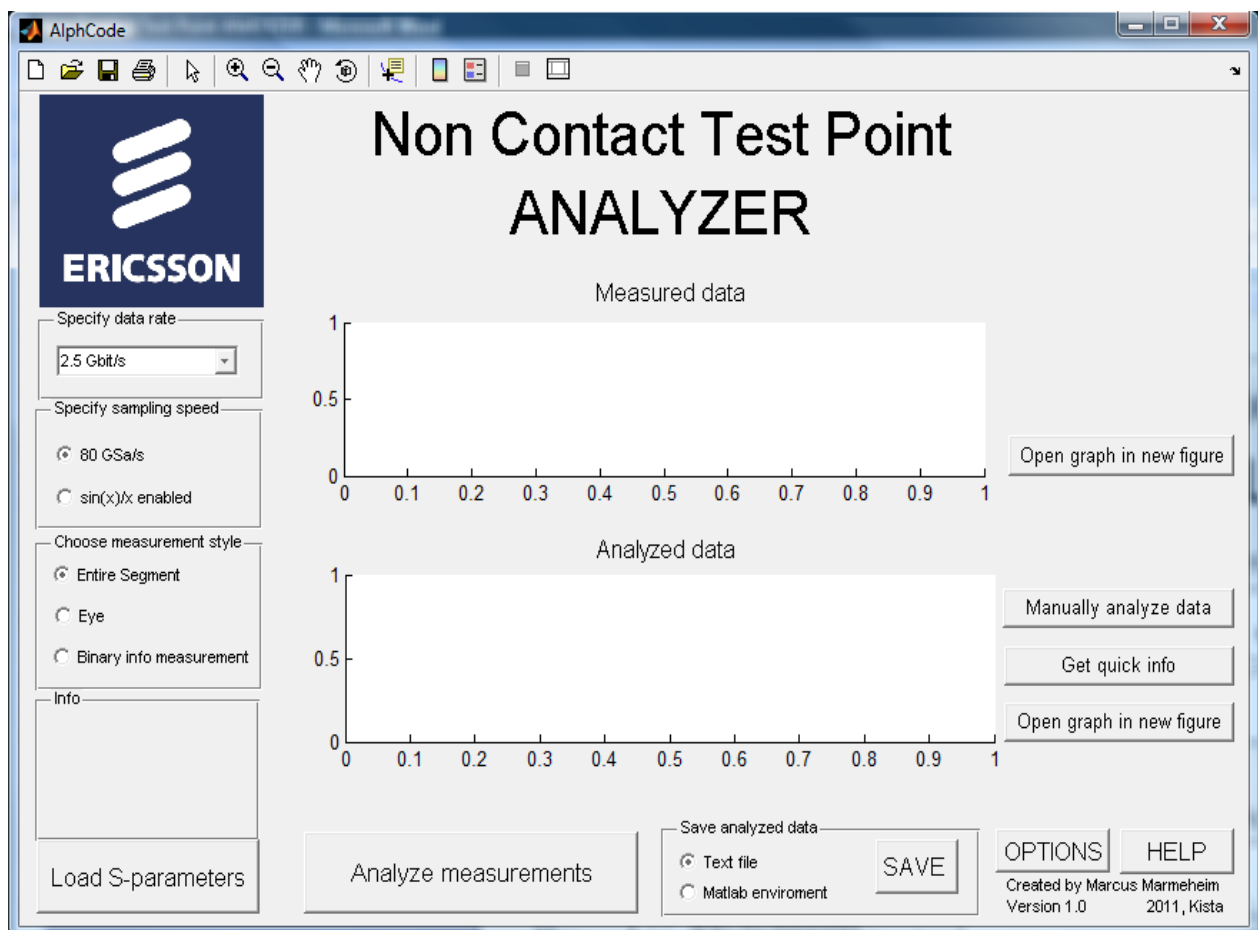
The text file should be stored in the folder *Measured data folder*, to minimize the risk of reading problems. As for the .s*p file; it may be retrieved from anywhere, so its location is not important.

LOADING THE S-PARAMETERS

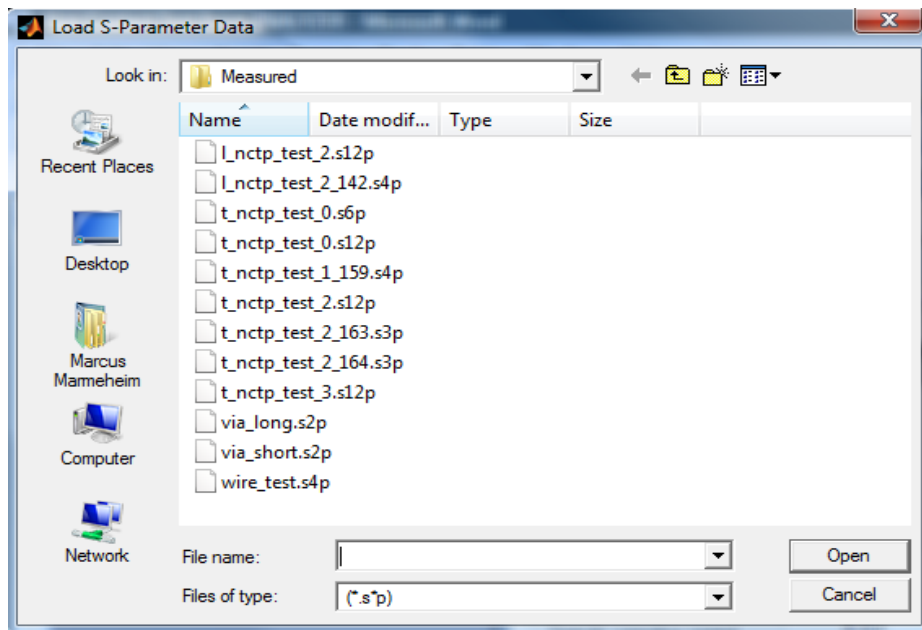
After all the preparations are done, simply click the applications icon named `nctp_analyzer` to start the program. This will open the DOS prompt, simply wait until the GUI pops up. It is also possible to start the program for DOS.

You should now be presented with the basic menu, with the default settings. Below is a screenshot of the interface. The program is now ready to be used.

For extra assistance, apart from this guide, you may click the **HELP** button in the bottom right corner of the window. This will bring up the help menu, containing quicker hints than this excessive guide.



The first thing that should be done is to load the correct `.s*p` file. This is done by clicking the **Load S-parameters** button and selecting the correct file, as shown below.



The program usually requires some time to fully load the information, do not click anything while waiting. If everything was done correctly and the file was of the correct format, the Info text box should now read Load successful. Do not be alarmed by the red color of the info text, every message will be displayed in this color.

SPECIFYING THE MEASUREMENT

First of all you need to select the measurement type, and this is done in the left corner of the screen on the panel Choose measurement type. There are three different types:

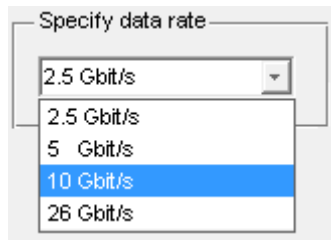
- Entire segment

This is the ordinary kind of analyzes; it simply reconstructs the original signal to the farthest possible extent. The output data will therefore have the same length as the input data. This option is selected by default.
- Eye

This option performs the same analyzes as the previous alternative, but it regroups the output data so that an eye pattern is generated.
- Binary info measurement

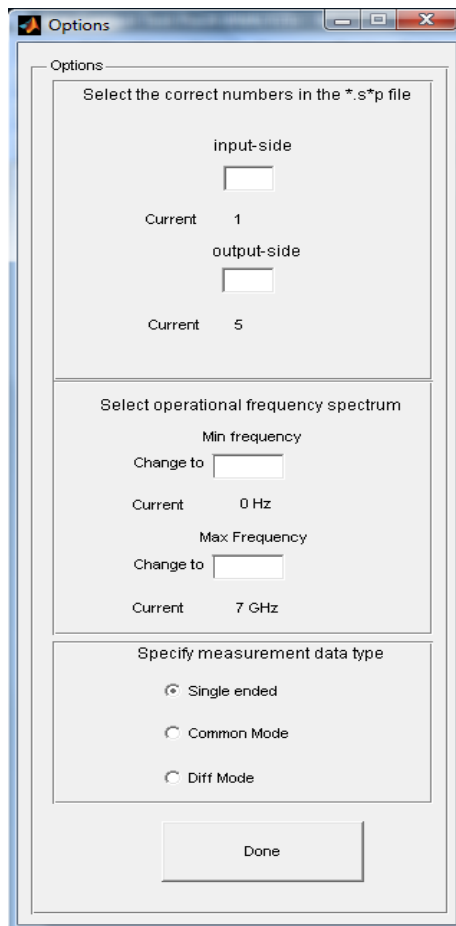
A binary measurement is an analysis that turns the signal into a binary code, i.e. ones and zeros. It still plots it along the same time axis as the Entire segment option, meaning that the length of the output data will be the same.

The next specification that may need to be changed made is the data rate of the measured signal. You will find the box right under the blue Ericsson logo. Just click it to bring forth the different alternatives. In version 1.0 of the Non Contact Test Point ANALYZER four different bit rates are available: 2.5, 5, 10 and 26 Gbit/s, as can be seen below



This specification is only important for the eye pattern and if the user wants to get the binary data. The user may experiment with this option to see the difference; as the code will guarantee an output for the “wrong” bit rate as well. Note: In case the predefined bit rates are not enough, more can easily be added; see further on in the guide for possible updates.

Further mandatory specifications that will need to be made are found by clicking the **OPTIONS** button on the bottom right corner of the window, right next to the **HELP** button. This will bring up the following window.

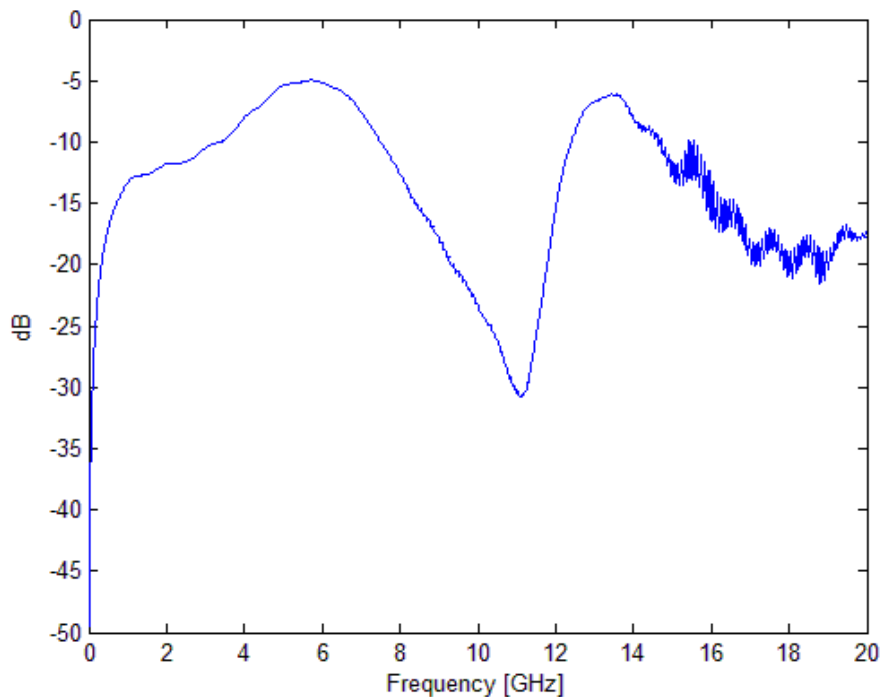


The first square asks for the numbers on the input and output sides of the *.s*p file. This refers to the position of the correct transfer function within the entire S matrix. For example: If the default values (seen as current in the figure) are used, this means that the marked transfer function within the following S matrix is the one in use

S_{11}	S_{12}	S_{13}	S_{14}	S_{15}
S_{21}	S_{22}	S_{23}	S_{24}	S_{25}
S_{31}	S_{32}	S_{33}	S_{34}	S_{35}
S_{41}	S_{42}	S_{43}	S_{44}	S_{45}
S_{51}	S_{52}	S_{53}	S_{54}	S_{55}

The horizontal position refers to the input side, while the vertical position (counted downwards) relates to the output side. Once you have written the correct number in one field, just hit enter and see the currently selected number change.

Since all operations upon the signal will be done in frequency domain, it is a good idea to see what the transfer function looks like in that domain. Most functions that will be used in this program hold a shape like the one below (i.e. it starts very close to zero and returns to a very small value later on), and not the entire spectrum is appropriate to use. Since the transfer function gets inverted during the reconstruction process; frequencies containing to small values risk being extremely sensitive to noise.



In the example above, it is appropriate to select a spectrum between 0 Hz and about 9.5 GHz. Usually signals are less sensitive to small values for low frequencies, and the software is designed to handle the situation of $S_{51}(0)=0$.

When you change the variables: always define them in Hz, even though the “current” value may be in GHz (or something else). This general rule applies to the entire program; always assign values in SI-units.

The third, and final, thing that needs to be done on this menu is to Specify measurement data type. The three options are

- **Single ended**
Single ended means that only the second column is used when analyzing the data (remember that the first one defines time), even though others may be present.
- **Common Mode**
This means that the first and the second columns are added together, effectively measuring any common mode signal that may be residing within them.
- **Diff Mode**
A Diff mode measurement means that the values from the third column are subtracted from the second, making an analysis on the signals as if they were a pair in differential mode.

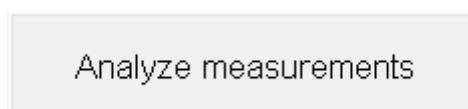
Should Common mode or Diff Mode be selected without an third column being present, the program will (before initiating the reconstruction) give a warning message and then proceed as if the Single ended mode was enabled.

These are the preparations that will need to be made before executing the reconstruction, simply click Done on the Options menu to close it. It should probably be mentioned that the order on which the specifications are made is irrelevant.

Note: in Version 1.0, the sampling speed does not need to be predefined. Instead the program will automatically obtain that parameter. This is a remain from an earlier version of the GUI.

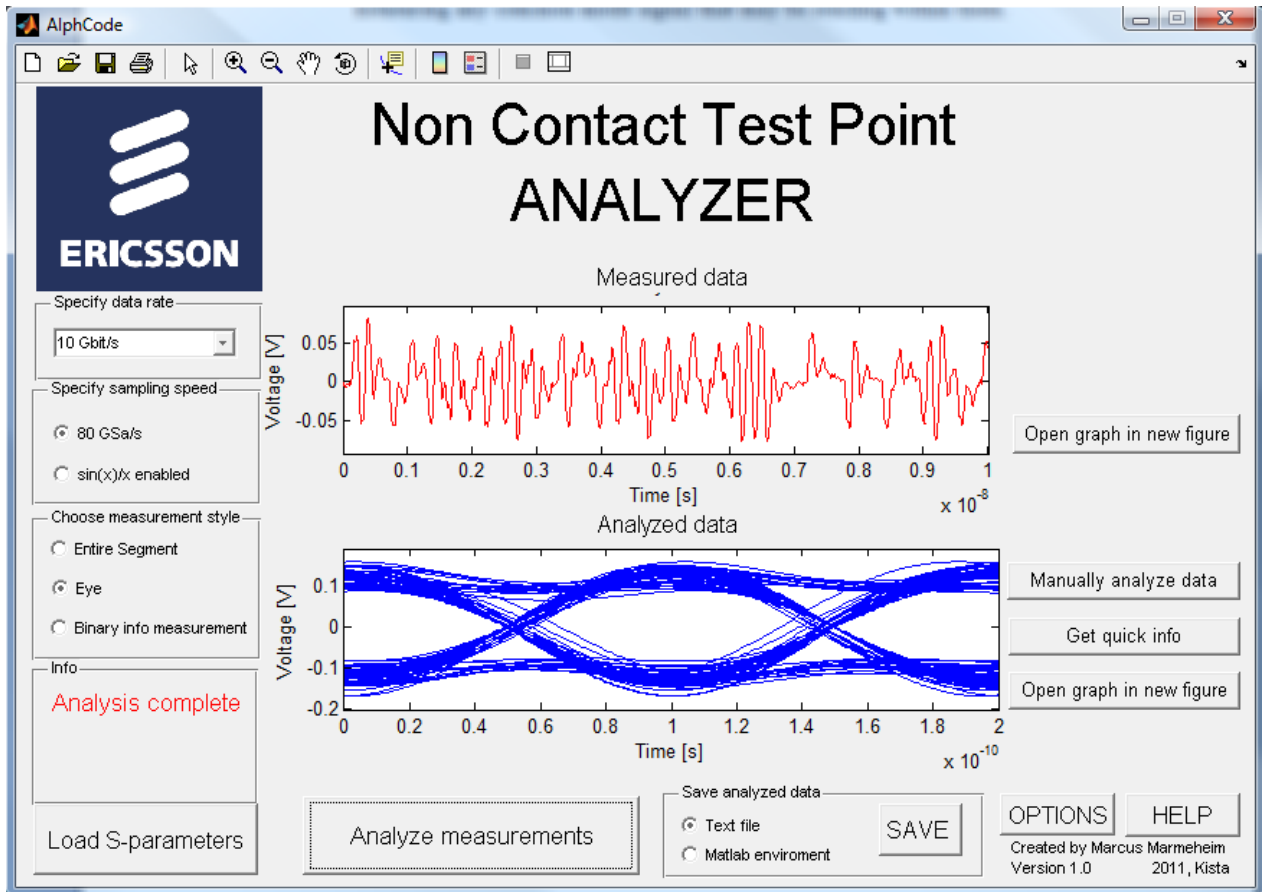
INITIATING AND PERFORMING THE ANALYSIS

Once everything has been prepared, and you have returned to the main menu, click the button on the lower part of the window that looks like this

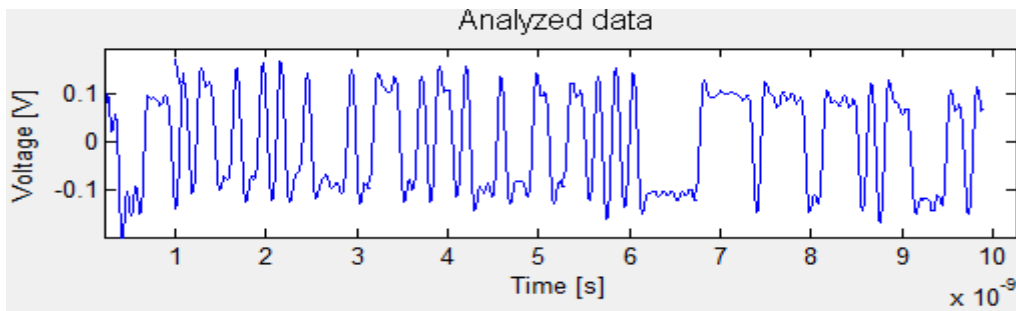


This will bring up a browser window. Just select the measurement file that you previously stored in the *Measured data folder* and click “ok” to initiate the procedure. As said earlier; the execution time is depending on the amount of data and the available processing power.

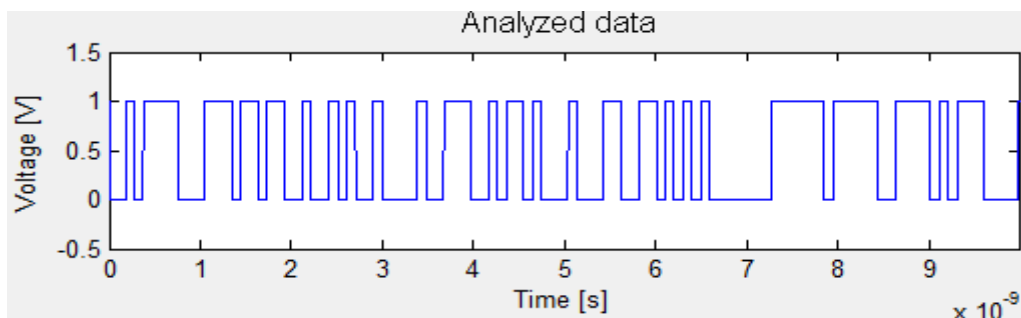
Unless something has gone wrong, the info text box will declare Analysis complete when the process is finished and the interface will look something like this (obviously depending on what choices you have made, and what input files you used).



The two empty plots have now been filled. On the upper one, colored red, is the original data (though a potential offset may have been removed), and on the lower plot is the analyzed data. In this particular scenario, a 10 Gbit/s signal was measured, and an eye pattern was generated. Had the Entire segment instead been selected, the second graph would have looked like this

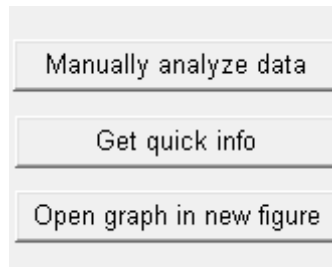


And the Binary info measurement would have looked something like this

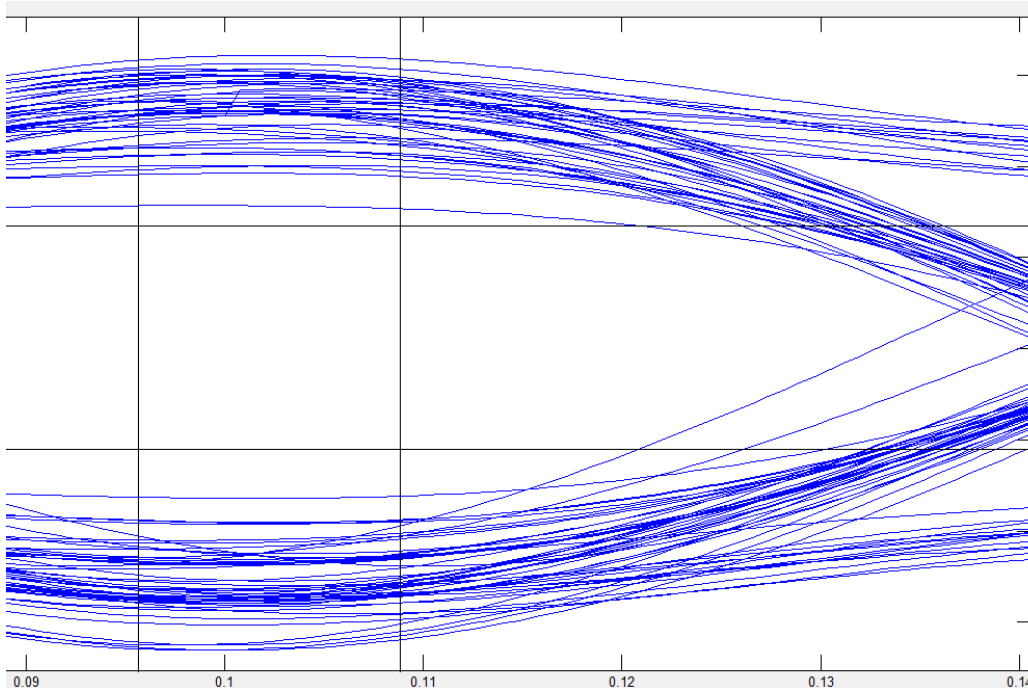


USING THE RECONSTRUCTED DATA

Right next to the second graph, there is a group of three buttons; they are all in some way used to operate upon the finished analysis. The three buttons look like this



The first one, Manually analyze data, will open up a huge window. The window is a little too big to show on a piece of A4 paper, so instead the important pieces are shown.



The main part of this window consists of a plot of the output data (regardless if it is entire segment, an eye pattern or binary info). In this case the eye pattern is included, as well as four additional black lines. These four lines can be moved, and placed anywhere on the plot. The two vertical lines will then give information about the time on each specific location, while the other two lines will give the user information about the voltage levels.

In the following square, in the bottom left corner, the functions for moving the lines are located as well as the measurements.

Select measurement lines

Click to update V1	Write to update V1	V1= 0.067345 V
Click to update V2	Write to update V2	V2= -0.055239 V
Click to update t1	Write to update t1	t1= 0.10884 ns
Click to update t2	Write to update t2	t2= 0.095667 ns

You are presented with two options; either specify the locations by writing or click on the plot. The values on the right side will update automatically.

There is another important text square present in the current window, and it contains new data that has been calculated using the data above.

Data

```

dv= -0.12258 V
dt= 0.013175 ns
1/dt= 75.8989 GHz
dw/dt= -9303.9984 MW/s

```

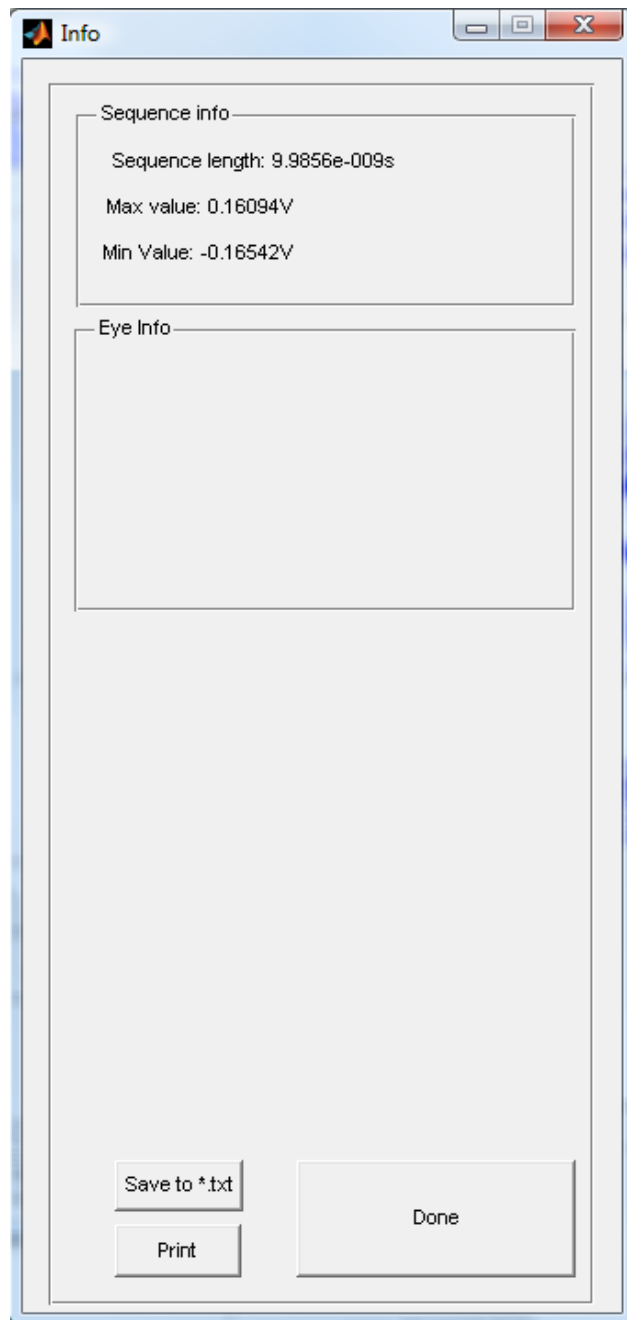
The four parameters here are easily calculated by the use of the four previous. Since most of them are self-explanatory, it will be up to you to make use of them. But one thing is important: dv is the $V2-V1$ (the difference in voltage between the lines) while dt is the absolute value of $t2-t1$ (a time interval should not be negative).

This window will be very useful when analyzing the data, providing you with extra information, such as derivatives. To close it; simply press the **DONE** button.

The next button

Get quick info

will open up a small text box that contains some information about the analyzed data. Exactly which information will depend on what type of measurement that has been made. The window looks like this, but apart from the Done button it does not contain any interactive features.



The third and final button Open graph in new figure opens up a standard MATLAB figure window. The advantage, compared to the window opened with **Manually analyze data** is that this window is more suitable for printing or saving. Granted, the standard MATLAB figure toolbar is included above every figure in the program. But on most operating systems; printing the shown figure will bring difficulties when a GUI is involved. With a standard figure window, those problems are avoided. This is what the standard toolbar looks like

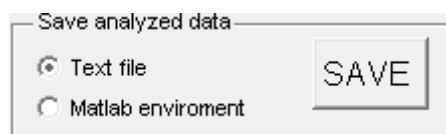


The icons for saving and printing are contained within the red rectangle, while the icons within the green will help you zoom and move around in the graphs.

STORING THE ANALYZED DATA

The saving icon described in the previous chapter only saves figures (i.e. the graphical representation of the data). A MATLAB GUI supports a huge amount of formats when saving figures; most common are probably *.bmp, *.png or *.jpg, but many more are available. There is one format alternative called MATLAB figure (*.fig), but you may want to avoid this one due to common conflicts with software from Microsoft (though the problem may be/have been solved in newer versions).

When it comes to saving the analyzed information, two different ways are available. In the bottom of the window you can see the following box



As you can see; the two alternatives are named Text file and Matlab environment. When you choose the first one, the program will store the saved data in a text file consisting of two columns (the exact same structure as a single ended input file) if you have made an entire measurement or a binary info measurement. If an eye pattern was generated, then the text file will consist of a matrix, where the first column is the time axis for the eye and the rest are different voltage figures.

Once you have pressed the SAVE button, and the save has been completed, the info box will read Data saved in AnalyzedData.txt. The text file will automatically be placed in the same folder as the program's *.exe file.

The other alternative will allow you to store it as an iddata object in MATLAB, ready to be used in the workspace. Iddata objects are part of the *signal processing* toolbox, so do not use this option if your MATLAB lacks the appropriate licenses. The data you supplied through the text input file will also be stored within this object. For more detailed information about iddata, please visit <http://www.mathworks.se/help/toolbox/ident/ug/bqt1uuy.html>. If the data is an eye pattern, the MATLAB object will instead be a matrix (and thereby not contain any information of the input).

Once you have selected the second radio button and pressed SAVE, you will be presented with a browser window that will prompt you to save the data as a *.mat file. Due to a bug in the MATLAB GUI, the file will always be saved in the same folder as the *.exe file, no matter where you try to place it.

When having loaded the file into the MATLAB workspace, the iddata object will be called writing Analyzed_data (for readers unfamiliar with MATLAB: a *.mat file may contain several different variables and their names are independent of the *.mat file's name.)

Keep in mind that this program always saves the last analyzed data, and that this version is not able to temporarily keep previous outputs in memory. So always save data directly once you have decided to keep it.

TROUBLESHOOTING/ Q&A

I get an error message after selecting the input file

Try checking the text file for redundant text objects (like names of the columns or notes at the end).

The program freezes when I try to select the S-parameters

On some systems, especially when other programs are running in the background, it will take some time to open the "Load S-Parameter data" browser. Try giving it some extra time before closing the application.

The program does not accept measured S-parameters, claiming that they are of a "not supported touchstone format"

This problem has appeared after measurements made on certain network analyzers and only data from a few ports are stored to the touchstone file. The easiest way around this problem is to resave the data, and let the file contain the measurements from every port (even the ones that are unconnected).

I wish to plot both the input and the output in the same figure, is this possible?

It is possible, but not in this GUI. You will have to import the data into MATLAB and plot the graphs there.

I used the figure toolbar to change the view of the data, and now I wish to return to the original

Double clicking the figure, with any tool used to manipulate the view, will automatically return you to the default setting.

The measured data that I use contain an offset, is this going to affect the results?

No, the program automatically compensates for a constant offset.

I copied the program application to my hard drive and the DOS prompt opens fine, but when the main window opens the program crashes instantly

If you just copy the application file the program will not start. You need also to include the bitmap file named Logo and the .mat file called settings.